IEEE Access
Multidisciplinary | Rapid Review | Open Access Journal

Received September 20, 2018, accepted October 12, 2018, date of publication October 22, 2018,
date of current version November 19, 2018.

Digital Object Identifier 10.1109/ACCESS.2018.2877402

An Improved S-Metric Selection Evolutionary Multi-Objective Algorithm With Adaptive Resource Allocation

ADRIANA MENCHACA-MÉNDEZ[1], ELIZABETH MONTERO[2,3], (Member, IEEE), AND SAÚL ZAPOTECAS-MARTÍNEZ[4], (Member, IEEE)

[1]Licenciatura en Tecnologías para la Información en Ciencias, ENES, Campus Morelia, National Autonomous University of Mexico, Morelia 58190, Mexico
[2]Departamento de Informática, Universidad Técnica Federico Santa María, Valparaíso 2390123, Chile
[3]Facultad de Ingeniería, Universidad Andres Bello, Viña del Mar 2531015, Chile
[4]Departamento de Matemáticas Aplicadas y Sistemas, Universidad Autónoma Metropolitana Unidad Cuajimalpa, Ciudad de México 05348, Mexico

Corresponding author: Adriana Menchaca-Méndez (adriana.menchacamendez@gmail.com)

The work of A. Menchaca-Méndez was supported by PAPIIT under Project IA105918. The work of E. Montero was supported by Fondecyt under Project 11150787.

ABSTRACT One of the main disadvantages of evolutionary multi-objective algorithms (EMOAs) based on hypervolume is the computational cost of the hypervolume computation. This deficiency gets worse either when an EMOA calculates the hypervolume several times or when it is dealing with problems having more than three objectives. In this sense, some researchers have designed strategies to reduce the number of hypervolume calculations. Among them, the use of the locality property of the hypervolume has emerged as an alternative to deal with this problem. This property states that if a solution is moving in its neighborhood, only its contribution is affected and the contributions of the rest of the solutions remain the same. In this paper, we present a novel evolutionary approach that exploits the locality property of the hypervolume. The proposed approach adopts a probability to use two or three individuals in its environmental selection procedure. In this way, it only needs to compute two or three hypervolume contributions per iteration. The proposed algorithm is evaluated by solving the standard benchmark test problems and two real-world applications where the features of the problems are unknown. According to the results, the proposed approach is a promising alternative for solving problems with a high number of objectives because of three main reasons: 1) it is competitive with respect to the state-of-the-art EMOAs based on hypervolume; 2) it does not need extra information about the problem (which is particularly essential when solving real-world applications); and 3) its computational cost is much lower than the other hypervolume-based EMOAs.

INDEX TERMS Evolutionary multi-objective algorithms, indicator-based EMOAs, hypervolume indicator.

I. INTRODUCTION

Many real-world problems involve the simultaneous optimization of a number of objective functions. Such problems are commonly known as multi-objective optimization problems (MOPs). In contrast to single-objective optimization problems where a unique solution is considered optimal, in multi-objective optimization, a set of solutions showing the best trade-offs among the objectives can be found. Throughout the years, evolutionary multi-objective algorithms (EMOAs) have become the preferred tool to deal with this type of problems. Notably, the nature of these algorithms (based on populations) makes possible to obtain multiple solutions to the problem. Consequently, a significant amount of research regarding the development of evolutionary approaches can be found in the specialized literature, see the comprehensive review presented in [1]–[3]. Such evolutionary approaches can be classified into three main groups: Pareto-based approaches (e.g., NSGA-II [4], SPEA2 [5]), decomposition-based methodologies (e.g., MOGLS [6], [7], MOEA/D [8], IM-MOEA [9]), and indicator-based algorithms (e.g., IBEA [10], SMS-EMOA [11]). Particularly, indicator-based EMOAs explicitly employ a performance indicator (e.g., hypervolume [12], $R2$ [13], $\epsilon_{+/*}$ indicator [14], *IGD* [15]) in their environmental selection procedures. Thus, since its introduction in the early 2000s, the indicator based evolutionary algorithm (IBEA) [10] marked

the beginning of a new generation of evolutionary approaches capable of solving, in a different way, problems with multiple objectives. To date, several evolutionary approaches based on performance indicators can be found in the specialized literature [10], [11], [16]–[19]. With their advantages and disadvantages, IBEAs constitute an amply line of investigation that in the last few years has been addressed by several authors. In the particular case of IBEAs adopting a reference set to compute the concerned performance indicator (e.g., $R2$, $\epsilon_{+/*}$, IGD, and their variants), are challenging to design because such reference set cannot be appropriately established. Nonetheless, several investigators have innovated different strategies to construct the reference set for this type of algorithms [16], [18]. On the other hand, hypervolume indicator [12] (as well referred to as S metric) has the advantage of not needing a reference set. Hypervolume indicator uses only a reference point which is much easier to state. This fact makes much more flexible the use of IBEAs based on hypervolume to deal with real-world problems where the features of the Pareto front are unknown. Although IBEAs based on hypervolume are flexible when solving multi-objective problems, their use is limited by the high computational cost of the hypervolume indicator which increases with the number of objectives.[1] As a consequence, an amply variety of research concerning the design of IBEAs based on hypervolume has been the subject of study in the last decade [11], [21]–[24]. So far, the development of hypervolume-based EMOAs is considered an active area of research into the evolutionary multi-objective optimization community.

In this paper, we introduce a new hypervolume-based EMOA that implements an adaptive control strategy to reduce the calculations of hypervolume contributions. In contrast to several hypervolume-based EMOAs which need to calculate all contributions to the hypervolume indicator per iteration, our proposed approach (namely iSMS-EMOA-ARA) only requires to compute two or three hypervolume contributions per iteration. We evaluate the proposed algorithm comparing its performance against two hypervolume-based EMOAs (namely iSMS-EMOA, and iSMS-EMOA II) which employ an environmental selection mechanisms similar to the one proposed in iSMS-EMOA-ARA. Besides, our proposed approach is compared against four state-of-the-art EMOAs based on different principles: GDE3, MOEA/D, NSGA3, and SMS-EMOA, on well-known multi-objective benchmark problems and two real-world applications. As we will see later on, our proposed iSMS-EMOA-ARA is an excellent alternative to deal with MOPs with distinct features, specially in problems with more than three objective functions.

The remainder of this paper is organized as follows. Section II introduces the basic concepts and terminology regarding evolutionary multi-objective optimization. It is followed by Section III which reviews the related work. The proposed approach is detailed in Section IV. A comprehensive study of the most critical parameter of our proposed algorithm is presented in Section V. The experimental studies on the well-known multi-objective benchmark problems and the two real-world applications are presented in Sections VI and VII, respectively. Finally, conclusions and some paths for future research are given in Section VIII.

[1] It cannot be computed precisely in polynomial time regarding the number of objectives unless $NP = P$ [20].

II. EVOLUTIONARY MULTI-OBJECTIVE OPTIMIZATION

A. MULTI-OBJECTIVE OPTIMIZATION PROBLEMS

Without loss of generality, a continuous box-constrained multi-objective optimization problem (MOP), assuming minimization problems, can be stated as:

$$\begin{aligned} &\textbf{minimize: } \mathbf{F}(\mathbf{x}) = (f_1(\mathbf{x}), f_2(\mathbf{x}), \ldots, f_M(\mathbf{x}))^T \\ &\text{s.t. } \mathbf{x} \in \Omega \end{aligned} \tag{1}$$

The vector function $\mathbf{F} : \Omega \to \mathbb{R}^M$ is composed by $M \geq 2$ scalar *objective functions* $f_i : \Omega \to \mathbb{R}$ $(i = 1, \ldots, M)$, where Ω denotes the feasible set which is implicitly determined by the box constraints of the problem, i.e., $\Omega = \prod_{i=1}^{n} [a_i, b_i]$.

In MOPs, there is no canonical order on $\mathbb{R}^M$, and thus, we need weaker definitions of order to compare vectors in $\mathbb{R}^M$. In this case, the *Pareto dominance relation* is usually adopted [25], [26]. The following definitions are introduced.

Definition 1 (Pareto Dominance Relation): We say that a solution vector $\mathbf{z}^1$ dominates the solution vector $\mathbf{z}^2$ (in the objective space), denoted by $\mathbf{z}^1 \prec \mathbf{z}^2$, if and only if:

$$\forall i \in \{1, \ldots, M\} : z_i^1 \leq z_i^2 \text{ and } \exists i \in \{1, \ldots, M\} : z_i^1 \prec z_i^2. \tag{2}$$

It is said that two vectors, $\mathbf{z^1}$ and $\mathbf{z^2}$, are mutually non-dominated vectors if $\mathbf{z^1} \not\prec \mathbf{z^2}$ and $\mathbf{z^2} \not\prec \mathbf{z^1}$. For $\mathbf{x^1}, \mathbf{x^2} \in \Omega$, we write $\mathbf{x^1} \prec \mathbf{x^2} \iff \mathbf{F}(\mathbf{x^1}) \prec \mathbf{F}(\mathbf{x^2})$.

Definition 2 (Pareto Optimality): A solution $\mathbf{x}^\star \in \Omega$ is Pareto optimal if there does not exist another solution $\mathbf{x} \in \Omega$ such that $\mathbf{F}(\mathbf{x}) \prec \mathbf{F}(\mathbf{x}^\star)$.

Definition 3 (Pareto Set): The Pareto optimal set (PS), is defined as: $PS = \{\mathbf{x} \in \Omega \mid \nexists\, \mathbf{y} \in \Omega : \mathbf{F}(\mathbf{y}) \prec \mathbf{F}(\mathbf{x})\}$.

Definition 4 (Pareto Front): For a Pareto optimal set PS, the Pareto front (PF), is defined as: $PF = \{\mathbf{z} = (f_1(\mathbf{x}), \ldots, f_M(\mathbf{x}))^T \mid \mathbf{x} \in PS\}$.

As in most of the multi-objective algorithms, we are interested in finding a finite number of elements of the Pareto optimal set, while maintaining a proper representation of the Pareto front.

B. EVOLUTIONARY APPROACHES FOR MULTI-OBJECTIVE OPTIMIZATION

Through the development of evolutionary algorithms for multi-objective optimization, various principles have been proposed. Such tenets involve different search strategies and methodologies that state the performance of a specific EMOA. Consequently, a considerable number of approaches based on these principles can be found in the specialized literature, see the comprehensive review reported

in [1]–[3]. Particularly, EMOAs can be classified into three main groups.

1) PARETO-BASED EMOAs

Initial evolutionary approaches for multi-objective optimization, integrate Pareto dominance relation to rank the population and assess closeness to the optimal Pareto front. Among the best known approaches for ranking solutions we found *dominance rank* [27], *dominance count* [5] and *dominance depth* [28]. However, a good approximation of the Pareto front has to fulfill two goals simultaneously: convergence and diversity. Therefore, to distribute the solutions along the entire trade-off curve, Pareto dominance has to be used in cooperation with a second criterion. Some methods have been proposed to distribute solutions along the Pareto optimal front include: *fitness sharing and niching* [29], *clustering* [5], *crowding distance* [4], among many others. Although EMOAs have amply adopted these methods in the first decade of the 2000s, their use has decreased. This is mainly due to two principal reasons: (i) the quick increase in the number of non-dominated solutions as we increase the number of objective functions, rapidly dilutes the effect of the selection mechanism of an EMOA [30] (many, even all solutions are equal) and (ii) the difficulty to measure diversity in a set of non-dominated solutions [31]–[35].

2) DECOMPOSITION-BASED EMOAs

In the last decade, scalarization functions have been employed by several evolutionary approaches giving rise to the well-known EMOAs based on decomposition. Decomposition approaches rely on solving a number of scalarizing functions which are formulated by an even number of weight vectors. Decomposition-based EMOAs have been found to be very efficient for solving complicated test problems (see for instance [8], [36], [37]). Additionally, by having a well-distributed set of weight vectors, a proper representation of the PF can be obtained by some EMOAs. However, because the unknown geometry of the Pareto front in real-world problems, the distribution of the weight vectors needs to be carefully defined. On the other hand, a well-distributed set of weight vectors in a many-objective scenario becomes difficult to obtain. These issues are the main disadvantages of this type of approaches when dealing with MOPs with difficult PF geometries [38], [39] or high-dimensional objective spaces [40].

3) INDICATOR-BASED EMOAs

Indicator-based EMOAs employ performance indicators in their environmental selection procedures. To date, there exist several indicators to assess convergence and diversity (or both at the same) of non-dominated solutions produced by EMOAs [14], [41], [42]. Particularly, a proper PF representation of a MOP can be reached by adopting the hypervolume indicator [12] or, if there exists an appropriate PF discretization of the MOP, indicators based on reference sets such as $R2$ [13], IGD [15], or Δ_p indicator [43]. Despite the difficult task of constructing a reference set to be employed in the search process of IBEAs, several researchers have innovated strategies for a proper construction of the reference set in this type of IBEAs, see the investigations reported for IGD/IGD$^+$ [44], R2 [45]–[47], and Δ_p indicator [16]–[18]. In contrast, hypervolume-based approaches only require a single reference vector to compute the hypervolume which results much more comfortable to estimate. Unfortunately, hypervolume-based IBEAs are limited by the high computational cost of the hypervolume indicator which increases as the number of objectives increases. Nonetheless, an advantage of using IBEAs based on hypervolume is that they can deal with different Pareto front geometries, including convex, concave, mixed, disconnected and degenerated shapes. It is worth noticing that the above approaches have difficulties when dealing with MOPs in high-dimensional objective spaces. In [48], Schutze *et al.* discussed the hardness to solve many-objective optimization problems.

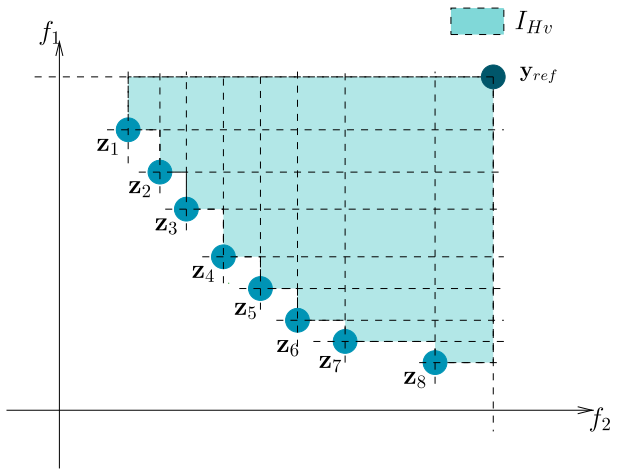

FIGURE 1. Hypervolume indicator. Let $\mathcal{A} = \{\mathbf{z}_1, \mathbf{z}_2, \cdots, \mathbf{z}_8\}$ be a set of non-dominated solutions and $\mathbf{y}_{ref}$ be a reference point. Then, the light blue area is the hypervolume of $\mathcal{A}$.

III. RELATED WORK

The hypervolume indicator (or S metric) was introduced in [12] to evaluate the performance behavior of EMOAs. It is defined as the space size covered by a set of non-dominated solutions (see Figure 1). Initially, this performance measure was adopted into the environmental selection procedure of the well-known IBEA [10]. IBEA estimates the hypervolume contribution of a solution by aggregating the pairwise hypervolume difference between the target solution and other solutions, as illustrated in Figure 2, where solution $\mathbf{z}_5$ has a lower hypervolume contribution than solution $\mathbf{z}_4$. Thus, solutions with less hypervolume contribution are removed from the current population. This idea of removing the worst solutions according to their hypervolume contributions has so far been employed in different ways by several researchers. Knowles and Corne [49] introduced a bounded external archive to store the non-dominated solutions found

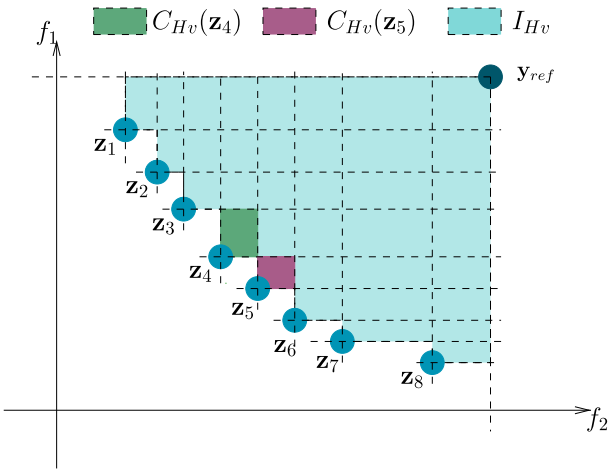

FIGURE 2. Hypervolume contribution. Let $\mathcal{A} = \{\mathbf{z}_1, \mathbf{z}_2, \cdots, \mathbf{z}_8\}$ be an approximation to the Pareto optimal set and $\mathbf{y}_{ref}$ be a reference point. Then, the green area is the hypervolume contribution of solution $\mathbf{z}_4$ because this area is only dominated by solution $\mathbf{z}_4$. Similarly, the pink area is the hypervolume contribution of solution $\mathbf{z}_5$.

throughout the search of an EMOA. If the number of allowed solutions is overcome, the archive is pruned by using Pareto ranking as the first criterion and the hypervolume contribution of each solution is employed as the second criterion. Analogously, Huband *et al.* [50] employed an evolution strategy based on hypervolume. The environmental selection procedure uses Pareto ranking as the primary selection criterion and the hypervolume contributions as a second selection criterion. Beume *et al.* [11] and Emmerich *et al.* [51] proposed the SMS-EMOA based on the NSGA-II [4] framework. SMS-EMOA generates only one offspring solution by iteration. Consequently, the environmental selection of SMS-EMOA applies Pareto ranking of NSGA-II. If the last front has more than one solution, SMS-EMOA uses the hypervolume contributions to discard the worst solution in the population. Igel *et al.* [52] extended the use of CMA-ES [53] to deal with multi-objective problems (the well-known MOCMA-ES). The environmental selection in MOCMA-ES uses Pareto ranking as a primary selection criterion and crowding distance as the second criterion. When Pareto ranking could no longer discard solutions (all solutions are non-dominated), the hypervolume contribution is used to remove solutions as in the strategies described above. Other techniques using similar methodologies of the above approaches can be found in [23], [24], [54], and [55]. Despite the design of the different hypervolume-based EMOAs reported in the literature, the high computational cost of the hypervolume computation continues being the main limitation of these evolutionary approaches. Nonetheless, to alleviate in somehow this problem, several strategies have been investigated. Some of these approaches are for instance the hypervolume by slicing objectives (HSO) [56], the recursive pruning of trees introduced by Fonseca *et al.* (FPL) [57], the quick hypervolume (QHV) of Russo and Francisco [58], and the walking fish group (WFG) hypervolume algorithm [59]. On the other hand, studies to obtain the hypervolume contribution of a solution without computing the exact hypervolume have also been studied by some researchers, see the strategies reported in [60]–[63]. The hypervolume computation is an NP-hard problem which cannot be computed in polynomial time [20], [61], [64]. As a consequence, several researchers have preferred to approximate the hypervolume instead of its exact computation. Examples of these approaches are the Monte Carlo sampling methods proposed by Bader *et al.* [22] and Bader and Zitzler [65] and the achievement scalarizing functions-based methodologies proposed by Ishibuchi *et al.* [66], [67]. Although these methods have reduced the computational time of IBEAs based on hypervolume, the performance quality of such approaches is compromised.

In [68], Menchaca-Mendez and Coello Coello pointed out an apparent disadvantage of most of the hypervolume-based EMOAs: they need to calculate the hypervolume contribution of all individuals in the population when all solutions in the population are non-dominated. This fact causes that these EMOAs require a considerable computation time in the search, even impractical in MOPs with more than five objectives. To address this weakness, Menchaca-Mendez and Coello Coello [68] proposed a new selection scheme that calculates three hypervolume contributions: (i) the new individual, (ii) its closest neighbor from the current population, and (iii) an individual chosen randomly from the current population. This is possible because of the locality property of the hypervolume indicator [69]. In a more recent work, Menchaca-Mendez *et al.* [70] studied the possibility of reducing the calculations of hypervolume contributions by discarding the selection of random individuals. To this end, they define a new parameter: the probability of using the randomly selected individual (p_{rsi}) which was tuned with the tuning method EVOCA [71]. As we mention before, hypervolume-based EMOAs are a viable alternative to solve real-world MOPs because they do not need extra information about the problem. In contrast, EMOAs based on reference sets or based on decomposition need the definition of additional components that cannot be adequately defined beforehand (e.g., the reference set and the weight vectors set). However, the main disadvantage of hypervolume-based EMOAs is their high computational cost. For this reason, in this paper, we focus our research on the design of a new framework which can be adapted to any hypervolume-based EMOA in order to reduce the effort involved in calculations of hypervolume contributions. As we will see later on, our proposed approach can approximate the Pareto front of a problem by calculating two or three hypervolume contributions per iteration. This, in fact, can significantly reduce the computational cost of hypervolume-based EMOAs on many-objective optimization problems.

In the following sections, we introduce the proposed hypervolume-based EMOA and the exhaustive empirical study that we carried out to justify the components stated in our proposed approach.

IV. PROPOSED APPROACH

As we mentioned in the above sections, most of IBEAs based on hypervolume indicator become inefficient because calculating the hypervolume contributions is computationally expensive. Two IBEAs suggest to reduce up to two or three contributions per iteration, instead of considering to compute the contributions of all individuals in the population (usually more than 100 individuals) are iSMS-EMOA [68] and iSMS-EMOA II [70].

iSMS-EMOA generates an individual at each iteration by using the crossover and mutation operators used by NSGA-II [4]. After that, iSMS-EMOA applies its environmental selection procedure by considering: 1) the hypervolume contribution of the new individual, 2) the hypervolume contribution of the nearest neighbor of the new individual, and 3) the hypervolume contribution of a randomly selected individual from the current population. Then, iSMS-EMOA removes the individual with the lowest contribution of the above-concerned individuals. This process is carried out by a determined number of iterations. When the new individual is competing with its nearest neighbor, the locality property of the hypervolume indicator is implicitly employed.

The idea behind iSMS-EMOA is to increase the hypervolume contribution of the solutions set by local movements between neighboring solutions. However, as pointed out in [68], there exist MOPs for which it is difficult to generate solutions in some regions of the objective space that could increase the hypervolume contribution of the solutions set. Therefore, if the new individual is located in these regions, it is better to retain both, i.e., the new solution and its nearest neighbor. For this reason, the randomly selected individual plays an important role. Following a similar idea, iSMS-EMOA II introduces a probability p_{rsi} to be considered in its environmental selection procedure. iSMS-EMOA II simulates to flip a heavy coin to decide if the randomly selected individual participates in the competition. To set the p_{rsi} value, iSMS-EMOA II defines two optimization problems. The first one is to **maximize:** $I_{Hv}(A)$ where I_{Hv} refers to the hypervolume indicator, and A is the current Pareto front approximation obtained by iSMS-EMOA II. The second objective is to **minimize:** $N_{CHv}(A)$ such that $I_{Hv}(A) > \epsilon$, where $N_{CHv}(A)$ is the number of computations of the hypervolume contributions required to obtain A and ϵ is the minimum required quality of A regarding I_{Hv}. In other words, iSMS-EMOA II minimizes the number of hypervolume computations N_{CHv} avoiding to affect strongly the hypervolume indicator I_{Hv} (i.e., the quality of solutions). The above optimization problems are solved by a suitable setting of parameter p_{rsi} which is tuned using EVOCA tuner [71].

The p_{rsi} values found by EVOCA for the second problem (i.e., the minimization problem) are shown in Table 1. The experimental tuning in iSMS-EMOA II was carried out adopting four MOPs taken from the DTLZ [72] test suite (DTLZ1, DTLZ2, DTLZ4, and DTLZ7) and three MOPs taken from the Walking-Fish Group (WFG) test suite [73] (WFG1, WFG2, and WFG4). The above MOPs were used by considering between three and five objective functions. These test problems have different characteristics: DTLZ1 has a linear PF, and it is multimodal. DTLZ2 and DTLZ4 have a concave PF, and they are unimodal but DTLZ4 tests EMOAs ability to maintain proper distribution of solutions. DTLZ7 has a disconnected PF. WFG1 is unimodal, but it has flat regions, and it is strongly biased towards small values of the variables, which makes very difficult its resolution. WFG2 is nonseparable and multimodal, and it has a disconnected PF. Finally, WFG4 has a concave PF, and it is highly multimodal.

TABLE 1. p_{rsi} values when iSMS-EMOA II minimizes the number of computations of the I_{Hv} contributions.

	$M = 3$	$M = 4$	$M = 5$
DTLZ1	0.222	0.144	0.240
DTLZ2	0.193	0.075	0.088
DTLZ4	0.020	0.000	0.184
DTLZ7	0.100	0.107	0.100
WFG1	0.400	0.149	0.124
WFG2	0.200	0.300	0.500
WFG4	0.100	0.000	0.127

Table 1 shows that each MOP needs a different value for p_{rsi}, i.e. the value of p_{rsi} strongly depends on the characteristics of the MOP (number of objective functions, geometry of PF, difficult landscapes, etc.). The latter is a significant disadvantage because it means that for each MOP it is necessary to set p_{rsi} with EVOCA, and it becomes even more expensive than calculating the contributions of all individuals in the population at each iteration of the algorithm. For this reason, in this work, we propose to implement an adaptive control strategy to vary the p_{rsi} value during the search process as follows:

- First, let N be the population size, then, one generation is completed after generating N offspring individuals.
- Second, the randomly selected individual (denoted by $\mathbf{x}_{rsi}$) is used to allow that both the new individual and its nearest neighbor survive. It is with the aim to improve diversity when the new individual is in a sparsely populated region. If an individual is randomly selected from the current population and there are highly populated regions, it is very probable that this individual is in one of these regions and then its hypervolume contribution will be small. When the three individuals compete (the new individual, its nearest neighbor, and a randomly selected individual), the randomly selected individual will lose, and the new individual and its nearest neighbor will survive in the population. Therefore, we say that the randomly selected individual is successfully employed if it allows that the new individual and its nearest neighbor survive.
- Third, the following probabilistic analysis is considered. Suppose that after generating N individuals, it is observed that $\mathbf{x}_{rsi}$ was successfully used during $p \times N$ times, i.e. p is the probability that $\mathbf{x}_{rsi}$ will be successful.

Therefore, if the same experiment is repeated but now using p_{rsi} to decide if $\mathbf{x}_{rsi}$ is employed at each competition, it is expected that $p_{rsi} \times p \times N$ times, $\mathbf{x}_{rsi}$ will be successfully employed. Then, the number of times that $\mathbf{x}_{rsi}$ was not used, and it could have been used successfully is $(1-p_{rsi}) \times p \times N$, i.e., if it is expected that $\mathbf{x}_{rsi}$ will be used successfully at least 90% of the times that it is successful, p_{rsi} should be equal to 0.9.

- Fourth, it is assumed that $\mathbf{x}_{rsi}$ is useful if it is successfully used in at least some percentage p_s of the times that it was employed.
- Fifth, if $\mathbf{x}_{rsi}$ is useful, it is wanted that $\mathbf{x}_{rsi}$ will be used the 100% of times that it was successful, and then p_{rsi} is equal to 1.0. Otherwise, $\mathbf{x}_{rsi}$ will be used for at least some percentage (*per*) of times that it was successful and *per* will decrease in a linear way. Therefore, it is proposed to set $p_{rsi} = ratio \times p$ at each generation where $p = \frac{x}{y}$, x is the number of times that $\mathbf{x}_{rsi}$ was successful and y is the number of times that $\mathbf{x}_{rsi}$ was used in the competition. *ratio* must be set according to the value of p_s, e.g. if it is considered that x_{rsi} is useful when p_s is at least 50% (i.e. $p \geq 0.5$), then *ratio* must be equal to 2.
- Sixth, the first generation always uses $p_{rsi} = 1.0$, and in next steps, the information of the previous generation is used to update the value of p_{rsi}. If $p_{rsi} > 1$, we set it to 1.0. If $p_{rsi} < 0.1$, we set it to 0.1. With this, the algorithm always makes use $\mathbf{x}_{rsi}$, even p_{rsi} can increase again if the search requires it.

Algorithm 1 shows the *Improved SMS-EMOA with Adaptive Resource Allocation* (iSMS-EMOA-ARA). To contrast the main differences with respect to iSMS-EMOA II, we highlight the additional steps in Algorithm 1. In line 1, control indicators are initialized. In line 5, a completed generation is identified and the p_{rsi} rate is updated. The control indicators x and y are updated in lines 15 and 23, respectively. Now a new question arises: what is the proper value for the *ratio* parameter? In the next section, we shall address this issue.

Algorithm 1 iSMS-EMOA-ARA

Input : p_c and η_c (parameters for the crossover operator), p_m and η_p (parameters for the mutation operator), N (size of the population), N_{gen} (maximum number of generations: it is considered a new generation after N iterations of the algorithm) and the MOP to be solved.

Output: A (the approximated Pareto front).

1 $p_{rsi} \leftarrow 1.0, x \leftarrow 1, y \leftarrow 1$;
2 Generate a random initial population (A);
3 $n \leftarrow 1$;
4 **while** $n <= N \cdot N_{gen}$ **do**
5 **if** $n \mod N = 0$ **then**
6 $p_{rsi} \leftarrow \min(1.0, ratio \cdot \frac{x}{y})$;
7 $p_{rsi} \leftarrow \max(p_{rsi}, 0.1)$;
8 $x \leftarrow 0, y \leftarrow 0$;
9 Select randomly two individuals from A ($\mathbf{x}_1$ and $\mathbf{x}_2$);
10 Obtain an offspring ($\mathbf{x}_{new}$) from $\mathbf{x}_1$ and $\mathbf{x}_2$, applying the operators of NSGA-II (crossover and mutation);
11 *nearest* $\leftarrow$ Index of the nearest neighbor to $\mathbf{x}_{new}$ in A;
12 $C_{Hv}^{new} \leftarrow$ hypervolume contribution of $\mathbf{x}_{new}$;
13 $C_{Hv}^{nearest} \leftarrow$ hypervolume contribution of $\mathbf{x}_{nearest}$;
14 **if** $rand(0, 1) < p_{rsi}$ **then**
15 $y \leftarrow y + 1$;
16 *random* $\leftarrow$ Index of a randomly selected individual from A (such that *nearest* $\neq$ *random*);
17 $C_{Hv}^{random} \leftarrow$ hypervolume contribution of $\mathbf{x}_{random}$;
18 **if** C_{Hv}^{new} *is better than* $C_{Hv}^{nearest}$ *or* C_{Hv}^{random} **then**
19 **if** $C_{Hv}^{random} > C_{Hv}^{nearest}$ **then**
20 Replace $\mathbf{x}_{nearest}$ with $\mathbf{x}_{new}$;
21 **else**
22 Replace $\mathbf{x}_{random}$ with $\mathbf{x}_{new}$;
23 $x \leftarrow x + 1$;
24 **else**
25 **if** $C_{Hv}^{new} > C_{Hv}^{nearest}$ **then**
26 Replace $\mathbf{x}_{nearest}$ with $\mathbf{x}_{new}$;
27 $n \leftarrow n + 1$;
28 **return** A;

A. COMPUTATIONAL COST

It is well known that computing the I_{Hv} indicator or the contribution to it has an exponential complexity [64]. Therefore, all hypervolume-based EMOAs have exponential complexity. However, the runtime required by each hypervolume-based EMOA can vary significantly. Let T_{Hv} and N be the time required to compute the hypervolume contribution and the population size of the hypervolume-based EMOA, respectively.

- Pioneers EMOAs based on hypervolume, such as SMS-EMOA, need to calculate N^2 hypervolume contributions per generation. Thus, each time that a new offspring solution is generated, the hypervolume contribution of each individual in the population is computed. Thus, the individual with the smallest hypervolume contribution is removed from the current population. Considering one generation when N offspring solutions are generated, the computational complexity of SMS-EMOA, per generation, is $O(N^2\ T_{Hv})$.
- iSMS-EMOA needs to calculate $3N$ hypervolume contributions per generation. Thus, each time that a new offspring solution is generated, it is necessary to compute the hypervolume contribution of the new solution, its closest neighbor, and a randomly chosen individual from the current population. Considering one generation when N offspring solutions are generated, the computational complexity of iSMS-EMOA, per generation, is $O(3NT_{Hv})$.

- iSMS-EMOA II and iSMS-EMOA-ARA can calculate less than $3N$ hypervolume contributions per generation. It depends on the parameters values that control such EMOAs (p_{rsi} for iSMS-EMOA II and *ratio* for iSMS-EMOA-ARA). In the case of iSMS-EMOA II, the parameter p_{rsi} is tuned with the tuning method EVOCA which implies to execute iSMS-EMOA II a number (K) of times. Considering one generation when N offspring solutions are generated, the computational complexity of iSMS-EMOA II, per generation, is $O(3NKT_{Hv})$. On the other hand, the parameter *ratio* in iSMS-EMOA-ARA is adaptively stated during the search. Therefore, iSMS-EMOA-ARA has a computational complexity, per generation, of $O(3NT_{Hv})$ which is much lower than the other hypervolume-based EMOAs.

V. STUDY OF *RATIO* PARAMETER

The purpose of these experiments is to validate the applicability of our approach on a variated of test problems reducing calculations of hypervolume contributions without deteriorating the quality of solutions.

For this task, we designed an experimental study to evaluate the significant deterioration in the quality of results concerning the reduction of hypervolume calculations produced by changes on the *ratio* parameter. In this scenario, a new multi-objective problem appears. The two objectives considered in this case are the maximization of hypervolume and minimization of calculations of hypervolume contributions. These two objectives are conditioned to the calibration of parameter *ratio*. Hence, we can consider it as a multi-objective tuning problem. In general, the hypervolume indicator and the number of hypervolume calculations increase as the *ratio* value increases.

To find the Pareto calibrations set to solve this multi-objective tuning problem we used MO-ParamILS [74] and the same MOPs used by iSMS-EMOA II. More precisely, we adopted four MOPs taken from the DTLZ [72] test suite (DTLZ1, DTLZ2, DTLZ4, and DTLZ7) and three MOPs taken from the Walking-Fish Group (WFG) test suite [73] (WFG1, WFG2, and WFG4). The concerning test problems were employed using between three and five objective functions. These test problems were selected because they have different features and it allows us to evaluate the proposed approach in several scenarios. In the next sections, we introduce MO-ParamILS tuning method used in our experiments, the concerned tuning scenarios, the results and conclusions of our adaptive approach.

A. MO-ParamILS

Tuning methods have demonstrated their ability to set parameter values for metaheuristics [75]. MO-ParamILS method is based on the well known ParamILS [76] approach. MO-ParamILS as ParamILs defines the dominance concept. In this case, it corresponds to the dominance concept defined in the multi-objective field: A parameter calibration **c** dominates a calibration **c'** if and only if **F(c)** dominates **F(c')**, with $\mathbf{F}(\cdot)$ the objective functions of the multi-objective tuning process.

MO-ParamILS executes an iterated local search process. Algorithm 2 shows its pseudocode. The process starts with a set of default parameter calibrations (line 1). These parameter calibrations are combined with a set of randomly generated calibrations (from lines 2 to 5). Dominated calibrations are removed during the archiving process. The set of non-dominated calibrations obtained from this process are used as initial archive (line 8).

At each iteration, a single parameter calibration from the current archive is selected (line 15). After a sequence of s 1-exchange modifications, the resulting calibration is stored as a new archive (line 18) from which the next local search phase starts. During the local search phase, all parameter calibrations are explored individually. All non-dominated calibrations found in their neighborhoods are added to the current set of solutions (line 19). MO-ParamILS also includes a restart probability that replaces the current archive by a randomly generated parameter calibration (lines 10 to 13).

In our experiments, we used the MO-FocusedILS version where comparisons between parameter calibrations consider both, the indicator quality and the number of executions required to reach it [76]. Additional executions were performed until either of two calibrations being compared dominates another. Intensification was promoted by increasing the number of executions of parameter calibrations. MO-ParamILS parameters where fixed according to authors recommendations: $r = 10$, $s = 3$, $p_{restart} = 0.01$.

B. MULTI-OBJECTIVE TUNING SCENARIO

In our experiments, we tuned the *ratio* parameter considering nine possible values between 1 and 20. We selected $ratio \in \{1, 2, 5, 8, 10, 12, 15, 18, 20\}$. A multi-objective tuning procedure was executed for each MOP to analyze the behavior of the proposed iSMS-EMOA-ARA in scenarios with different features. As stopping criteria, we considered a maximum effort of executions of parameter calibrations on the approximated Pareto calibrations set of 300 runs. This budget was set to limit the effort according to the cost of comparing all these parameter calibrations using 30 different random seeds.

Figs. 3–9 show the Pareto calibration fronts found on each studied MOP considering between three and five objective functions. Since we aim to maximize the hypervolume, we minimize $-I_{Hv}$. Also, we normalized the hypervolume values to fit plots with 3, 4, and 5 objectives in the same figures. From these figures, we can see that in almost all the test problems high values for *ratio* imply a higher hypervolume value but also a higher number of calculations of hypervolume contributions. On the other hand, low values for *ratio* imply savings of calculations of hypervolume contributions but compromising the quality of solutions. Therefore, we can conclude that effectively these two objective functions (i.e., maximize I_{Hv} and minimize N_{CHv}) are in conflict.

Algorithm 3 MO-ParamILS

Input : Initial archive A_i, parameters r (number of tries to generate random parameter calibrations), s (number of random perturbations of parameter calibrations) and $p_{restart}$ (probability of restart the tuning process.)

Output: A_{curr} (the approximated Pareto calibrations set).

$A_{curr} \leftarrow$ initial set of parameter calibrations;
for $i \leftarrow 1 \ldots r$ **do**
  $c \leftarrow$ random parameter calibration;
  update(A_{curr}, c);
  archive(A_{curr}, c);
repeat
  if *first iteration* **then**
    $A' \leftarrow A_{curr}$;
  else
    if $p_{restart}$ **then**
      $c \leftarrow$ random parameter calibration;
      $A_{curr} \leftarrow \{c\}$;
      $A' \leftarrow A_{curr}$;
    else
      $c \leftarrow$ random calibration from A_{curr};
      for $i \leftarrow 1 \ldots s$ **do**
        $c' \leftarrow$ random neighbor of c;
      $A' \leftarrow \{c'\}$;
  $A \leftarrow$ local search (A');
  for $c \in A$ **do**
    update(A_{curr}, c);
    archive(A_{curr}, c);
until *termination criterion is met*;
return A_{curr};

In DTLZ7 with 3, 4, and 5 objectives, WFG2 with 3 and 4 objectives, and WFG4 with 4 objectives, MO-ParamILS obtained a single solution in each Front with a ratio equal to 1. This means that for these MOPs the use of the randomly selected individual is significant at the beginning of the search but probably its relevance decreases quickly and, at the end of the search, the randomly selected individual is not useful. Only in WFG2 with 5 objectives, MO-ParamILS obtained a single ratio equal to 20. This means that in this MOP it is necessary the use of the randomly selected individual during the entire search process.

For problems in which there was a conflict between maximizing the hypervolume indicator and minimizing the calculations of hypervolume contributions, we can consider that these two objectives have the same importance and thus, we can select the solution in the knee or close to the knee of the Pareto calibrations front. For DTLZ1, DTLZ2, and WFG1 solutions with *ratio* equal to 2 or 5 were close to the knee (see Figs. 3, 4, and 7) . For DTLZ4, solutions with *ratio*

	M	$N_{CHv}(A)$	$-I_{Hv}$	$ratio$
DTLZ1	3	125619	−1.0	18
		124880	−0.99995	8
		124145	−0.99986	5
		121582	−0.99984	2
		116466	−0.99874	1
	4	121992	−1.0	8
		119885	−0.99996	5
		114471	−0.99968	2
		110640	−0.99899	1
	5	121010	−1.0	10
		117369	−0.99997	5
		112265	−0.99949	2
		109421	−0.99058	1

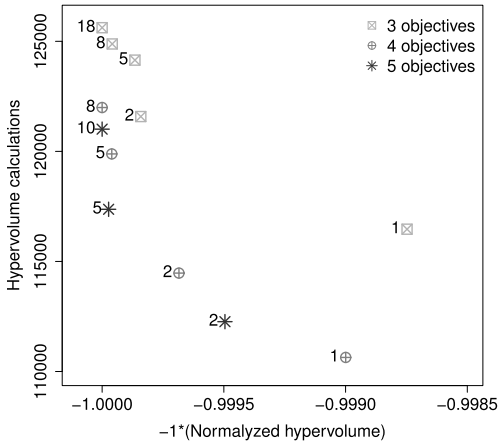

FIGURE 3. Pareto calibrations fronts of DTLZ1.

equal to 5 or 8 were close to the knee (see Fig. 5). Finally, for WFG4, solutions with *ratio* equal to 1 or 2 were close to the knee (see Fig. 9). From this, we can say that it is a good choice to use a *ratio* $=$ 5 for all MOPs because with this value, we can obtain a solution near to the knee or even above it, i.e., we can obtain a better quality in the Pareto calibrations front. DTLZ4 with 5 objectives was the unique exception because its *ratio* value was below the knee but above of the calibration with the worst hypervolume value. In this way, we can use a *ratio* $=$ 5 for any MOP and then we can save calculations of the hypervolume contribution because the user should not provide this parameter.

C. BEHAVIOR OF iSMS-EMOA-ARA

In Section V-B, we concluded that it is possible to use a *ratio* value equal to 5 for solving any MOP. Since *ratio* value is used to adjust the parameter p_{rsi} as the search progress. Figs. 10 and 11 show the convergence plots for this parameter in all test MOPs, using 3, 4, and 5 objective functions. In these plots, we can see that as the search progresses the value of p_{rsi} decreased, i.e., the randomly selected individual is less useful as the search continues. This remark is crucial because it corroborates the study presented in [68].

	M	$N_{CHv}(A)$	$-I_{Hv}$	$ratio$
DTLZ2	3	108353	−1.0	18
		106646	−0.99999	2
		105883	−0.99996	1
	4	107729	−1.0	8
		107232	−0.99991	5
		106106	−0.99984	2
		105438	−0.99969	1
	5	121010	−1.0	12
		117369	−0.99976	5
		112265	−0.99957	1

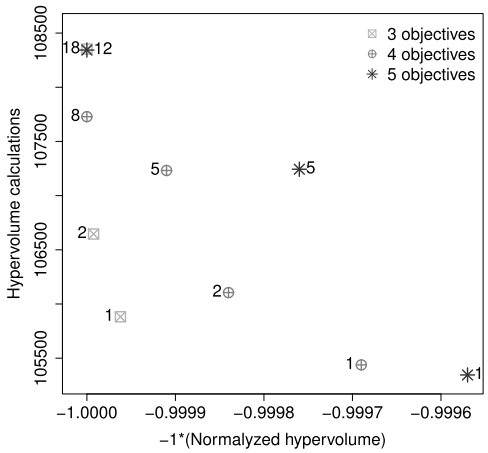

FIGURE 4. Pareto calibrations fronts of DTLZ2.

	M	$N_{CHv}(A)$	$-I_{Hv}$	$ratio$
DTLZ4	3	108169	−1.0	18
		107978	−0.99995	12
		107375	−0.99993	5
		105893	−0.99990	1
	4	107864	−1.0	15
		107771	−0.99997	12
		107476	−0.99990	8
		107013	−0.99986	5
		105397	−0.99974	1
	5	108005	−1.0	20
		107389	−0.99988	8
		105247	−0.99970	1

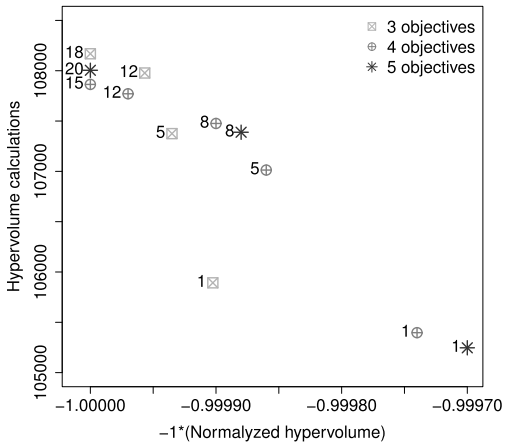

FIGURE 5. Pareto calibrations fronts of DTLZ4.

Another important behavior to observe is that the speed with which p_{rsi} decreased depends on the MOP being solved, e.g., for DTLZ1 the value of p_{rsi} stayed above 0.5 during the first 200 generations and reached a value of 0.1 around to generation 350. However, for DTLZ2, DTLZ4, and DTLZ7, p_{rsi} reached a value equal to 0.1 at generation 100 approximately. This behavior can be explained because DTLZ1 is highly multimodal and it is known that it generates many weakly dominated solutions. In WFG1, we can observe a different behavior because p_{rsi} varied between 0.1 and 0.25 constantly during most of the search. Also, this remark is important because, in WFG1, it is difficult to generate solutions in some areas of the PF, so it was expected that the role of p_{rsi} would be significant and the observed behavior reflected this difficulty. WFG2 has a similar behavior than WFG1, p_{rsi} varied between 0.1 and 0.3 from generation 50 to generation 300 and between 0.1 and 0.2 at the end of the search. Finally, in WFG4 we can observe that in the first 200 generations the value of p_{rsi} was also going up and down, but for the last 300 generations it was more stable.

Therefore, we can conclude that our proposal to adjust p_{rsi} during the search is successful because it can deal with different types of MOPs and it does not need extra information (we can use a ratio equal to 5 for any problem).

TABLE 2. Recommended values for parameters for iSMS-EMOA-ARA.

p_c	η_c	p_m	η_m	N	N_{gen}	$ratio$
0.9	15	$1/n$	20	100	500	5

VI. EXPERIMENTAL STUDY

In this section, we compare the proposed iSMS-EMOA-ARA regarding the iSMS-EMOA and iSMS-EMOA II which are two algorithms that adopt the local property of hypervolume to reduce the number of hypervolume computations. Our experimental study was carried out by performing 30 independent runs for each EMOA on the test problem under consideration. For all EMOAs, we adopted the Simulated-Binary Crossover (SBX) and the Polynomial-Based Mutation (PBM) mutation used by NSGA-II [4]. Table 2 shows the parameters used by iSMS-EMOA-ARA. p_c, η_c, p_m and η_m are parameters of crossover and mutation operators, respectively. Since they are taken from NSGA-II, we use the values suggested by its authors [4]. N and n denote the population size and the number of decision variables, respectively. It is well known that SMS-EMOA needs to compute N^2 hypervolume contributions per generation. Therefore, the time consumption of this algorithm became extremely high using large

	M	$N_{CHv}(A)$	$-I_{Hv}$	*ratio*
DTLZ7	3	107980	−1.0	1
	4	107035	−1.0	1
	5	106671	−1.0	1

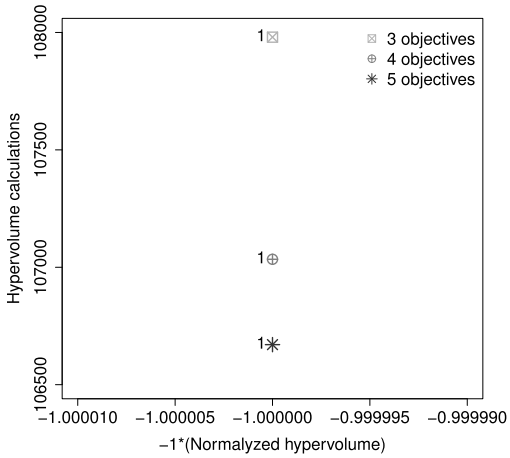

FIGURE 6. Pareto calibrations fronts of DTLZ7.

	M	$N_{CHv}(A)$	$-I_{Hv}$	*ratio*
WFG1	3	112616	−1.0	12
		111005	−0.98696	8
		109221	−0.97714	5
		106587	−0.96190	2
		105405	−0.94813	1
	4	114749	−1.0	15
		110076	−0.98689	5
		105502	−0.98045	1
	5	113788	−1.0	10
		110269	−0.99982	5
		106854	−0.99860	2
		105495	−0.99532	1

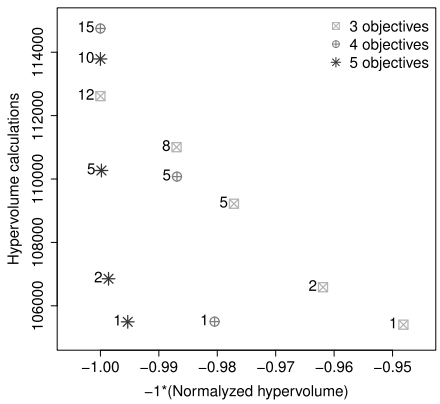

FIGURE 7. Pareto calibrations fronts of WFG1.

	M	$N_{CHv}(A)$	$-I_{Hv}$	*ratio*
WFG2	3	107426	−1.0	1
	4	106637	−1.0	1
	5	114194	−1.0	20

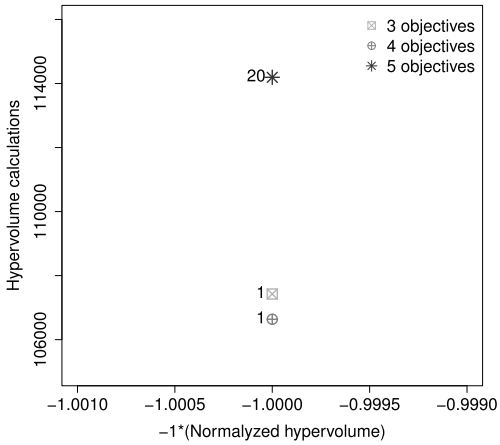

FIGURE 8. Pareto calibrations fronts of WFG2.

	M	$N_{CHv}(A)$	$-I_{Hv}$	*ratio*
WFG4	3	107710	−1.0	8
		105679	−0.99901	2
		105153	−0.99738	1
	4	105167	−1.0	1
	5	108969	−1.0	8
		105863	−0.99903	2
		105186	−0.99903	1

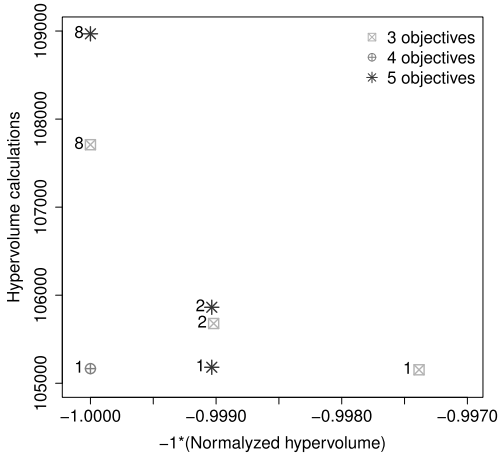

FIGURE 9. Pareto calibrations fronts of WFG4.

populations. As we consider meaningful the comparison of iSMS-EMOA-ARA against a symbolic hypervolume-based EMOA such as SMS-EMOA, we use $N = 100$ as shown in Table 2. N_{gen} is the number of generations performed by each algorithm. We use $N_{gen} = 500$ because the adopted test problems need at least 50,000 fitness function evaluations to find an approximate PF with good quality. Finally, *ratio* is a parameter exclusively used by iSMS-EMOA-ARA, the experiments reported in Section V indicate that 5 is

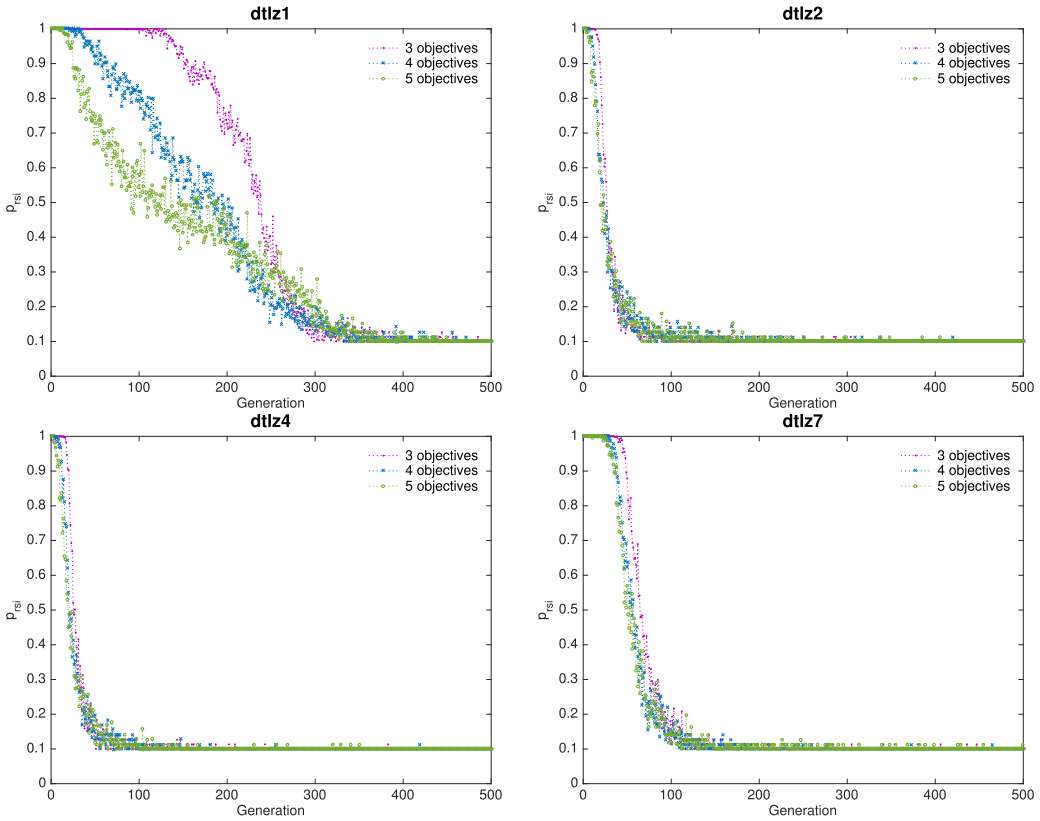

FIGURE 10. p_{rsi} **convergence in DTLZ test problems: Mean of 30 independent runs (in iSMS-EMOA-ARA) at each generation.**

a suitable value for this parameter. We used the same values for p_c, η_c, p_m, η_m, N and N_{gen} for all EMOAs under comparison.

A. ADOPTED TEST PROBLEMS

In our experimental study, we employed the test problems adopted in the adjustment of the *ratio* parameter. In this regard, we employed four test problems taken from the Deb-Thiele-Laumanns-Zitzler (DTLZ) test suite [72] (DTLZ1, DTLZ2, DTLZ4, and DTLZ7) using standard parameters, i.e., $k = 5$ for DTLZ1 and $k = 10$ for the rest of the problems. Additionally, we adopted three test problems taken from the WFG toolkit [73] (WFG1, WGF2, and WGF4) using standard parameters, i.e., $k_{factor} = 2$ and $l_{factor} = 10$.

B. PERFORMANCE INDICATORS

In the specialized literature, we can find a wide variety of performance indicators to evaluate the performance of EMOAs. However, it is worth noticing that the use of reference-based indicators (e.g., IGD, Δ_p indicator, etc.) requires a discretization of the real PF. Since we are evaluating the performance of our proposed approach in many-objective problems, the construction of a proper PF discretization is by itself a hard problem. Instead, the hypervolume indicator and the C-metric do not require the real PF, and they are Pareto compliant (i.e., they perfectly hold with the Pareto optimality) being a high advantage against reference-based indicators which are not compliant concerning Pareto optimality. For these reasons, we evaluate the performance of the proposed iSMS-EMOA-ARA using these two performance indicators.

1) HYPERVOLUME INDICATOR

The hypervolume performance indicator (I_{Hv}) was introduced in [12] to assess the performance of EMOAs. This performance indicator is Pareto compliant [14], and quantifies both proximity and distribution of non-dominated solutions along the PF. The hypervolume corresponds to the non-overlapped volume of all the hypercubes formed by a reference point $\mathbf{y}_{ref}$ (given by the user) and each solution $\mathbf{z}$ in the PF approximation (A). Hypervolume indicator is mathematically stated as:

$$I_{Hv}(A) = \mathcal{L}\left(\bigcup_{\mathbf{z}\in A}\{\mathbf{x}|\mathbf{z} \prec \mathbf{x} \prec \mathbf{y}_{ref}\}\right) \tag{3}$$

where $\mathcal{L}$ denotes the Lebesgue measure and $\mathbf{y}_{ref} \in \mathbb{R}^M$ denotes a reference vector being dominated by all solutions in A.

In our experimental study, the I_{Hv} indicator was computed on the normalized PF approximation achieved by an EMOA. The normalization of the PF approximation was carried out by considering all the PF approximations reached by the EMOAs

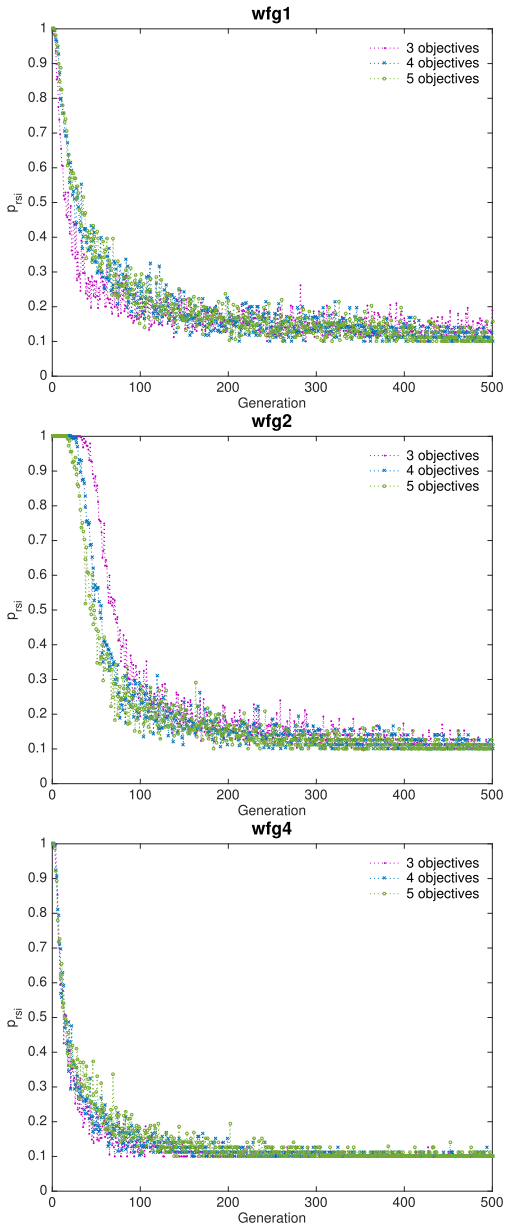

FIGURE 11. p_{rsi} **convergence in WFG test problems: Mean of 30 independent runs (in iSMS-EMOA-ARA) at each generation.**

on the test problem under consideration. Thus, we employed $\mathbf{r} = (1.1, \ldots, 1.1)$ as reference point.

2) SET TWO COVERAGE

The *Set Two Coverage* (or C-metric) was proposed by Zitzler *et al.* [77], and it compares a set of non-dominated solutions A with respect to another set B, using Pareto dominance. This performance measure is defined as:

$$\mathcal{C}(A, B) = \frac{|\{b \in B | \exists a \in A : a \preceq b\}|}{|B|} \tag{4}$$

If all points in A dominate or are equal to all points in B, this implies that $\mathcal{C}(A, B) = 1$. Otherwise, if no point of A dominates some point in B then $\mathcal{C}(A, B) = 0$. When $\mathcal{C}(A, B) = 1$ and $\mathcal{C}(B, A) = 0$ then, we say that A is better than B. Since the Pareto dominance relation is not symmetric (i.e. not always $\mathcal{C}(A, B) = \mathcal{C}(B, A)$ is held), we need to calculate both $\mathcal{C}(A, B)$ and $\mathcal{C}(B, A)$.

C. DISCUSSION OF RESULTS

In our comparative study, we elaborated a statistical analysis using Wilcoxon's rank sum to determine how an algorithm statistically outperforms another one (the null hypothesis "medians are equal" can be rejected at the 5% level, $H = 1$) and how they have a similar behavior (the null hypothesis cannot be rejected at the 5% level, $H = 0$). It is worth noticing that this statistical test was applied to compare two related samples, i.e., the results obtained by two different algorithms. As we aim to compare the proposed iSMS-EMOA-ARA regarding the state-of-the-art algorithms, we applied this statistical test between iSMS-EMOA-ARA and each EMOA adopted in our comparative study. In the results tables (Tables 3 and 4), we added a column per each adopted EMOA and we labeled this column as $P(H)$. In all the tables, the best results are in boldface font. If the cell corresponding to Algorithm A has a darker background than the cell corresponding to Algorithm B and $H = 1$, it means that Algorithm A obtained better results than Algorithm B. In the case of $H = 0$, it means that both algorithms have similar behavior.

Concerning iSMS-EMOA, we can see that in eleven problems iSMS-EMOA obtained better results than iSMS-EMOA-ARA regarding the hypervolume indicator. Nonetheless, the proposed iSMS-EMOA-ARA had a similar behavior to iSMS-EMOA in ten test problems. In Table 3, we can observe that in DTLZ1, DTLZ7, WFG2, and WFG4 test problems, iSMS-EMOA-ARA achieved a similar behavior to iSMS-EMOA. As we saw in the study of the parameter *ratio* (Section V), the impact of the randomly selected individual in DTLZ7 test problem was not significant in all generations. Therefore, it is natural to have similar behavior in this test problem for both EMOAs. On the other hand, it is well know that DTLZ1 and WFG4 are highly multimodal, and then, it is expected that an adequated use of the randomly selected individual could avoid getting stuck in local optima. Thus, we can say that the proposed iSMS-EMOA-ARA suitably adjusted the p_{rsi} value. If we look at Table 4, we can see that iSMS-EMOA-ARA saved from 16.47% to 28.64% the computation of the hypervolume contributions, i.e., it saved from 24,656 to 42,874 hypervolume calculations. For MOPs having five objectives (or more), this could decrease the runtime up to an order of hours.

Regarding iSMS-EMOA II, we can observe that iSMS-EMOA II and iSMS-EMOA-ARA had similar behavior in twelve problems. On the other hand, iSMS-EMOA-ARA was better than iSMS-EMOA II in seven test problems, and iSMS-EMOA II was better in two test problems. Although Table 4 shows that iSMS-EMOA II saved a higher amount of computations of the hypervolume contributions

TABLE 3. Results obtained by iSMS-EMOA, iSMS-EMOA II, and iSMS-EMOA-ARA regarding I_{Hv}. We show average values over 30 independent runs. The values in parentheses correspond to the standard deviations. $P(H)$ shows the results of statistical analysis applied to our experiments using Wilcoxon's rank sum and considering I_{Hv}. P is the probability of observing that the null hypothesis "medians are equal" is true. $H = 1$ indicates that the null hypothesis can be rejected at the 5% level.

f	iSMS-EMOA		iSMS-EMOA II min N_{CHv}			iSMS-EMOA-ARA
	I_{Hv}	$P(H)$	I_{Hv}	p_{rsi}	$P(H)$	I_{Hv}
DTLZ1 (3)	**1.12295 (0.00039)**	0.079 (0)	1.05915 (0.10386)	0.222	**0.000 (1)**	1.12278 (0.00046)
DTLZ2 (3)	**0.75792 (0.00009)**	**0.025 (1)**	0.75783 (0.00010)	0.193	0.420 (0)	0.75786 (0.00010)
DTLZ4 (3)	**0.98154 (0.00005)**	**0.000 (1)**	0.98111 (0.00021)	0.020	**0.000 (1)**	0.98147 (0.00007)
DTLZ7 (3)	0.56000 (0.03266)	0.149 (0)	**0.57499 (0.00046)**	0.100	**0.007 (1)**	0.55436 (0.03711)
DTLZ1 (4)	**1.37370 (0.00040)**	0.695 (0)	1.35296 (0.01729)	0.144	**0.000 (1)**	1.37362 (0.00049)
DTLZ2 (4)	**1.04430 (0.00017)**	**0.000 (1)**	1.04383 (0.00021)	0.075	**0.030 (1)**	1.04395 (0.00019)
DTLZ4 (4)	**1.40598 (0.00002)**	**0.000 (1)**	1.40536 (0.00014)	0.000	**0.000 (1)**	1.40593 (0.00004)
DTLZ7 (4)	0.56533 (0.01359)	0.663 (0)	**0.57349 (0.00192)**	0.107	0.056 (0)	0.56013 (0.02350)
DTLZ1 (5)	**1.60721 (0.00002)**	**0.005 (1)**	1.60403 (0.00500)	0.240	**0.000 (1)**	1.60719 (0.00002)
DTLZ2 (5)	**1.29568 (0.00017)**	**0.000 (1)**	1.29504 (0.00031)	0.088	**0.041 (1)**	1.29522 (0.00029)
DTLZ4 (5)	**1.29587 (0.00019)**	**0.000 (1)**	1.29537 (0.00026)	0.184	0.610 (0)	1.29541 (0.00026)
DTLZ7 (5)	**0.54870 (0.00438)**	0.167 (0)	0.54821 (0.00420)	0.100	0.252 (0)	0.54704 (0.00574)
WFG1 (3)	**1.21852 (0.01050)**	**0.000 (1)**	1.19464 (0.03315)	0.400	**0.001 (1)**	1.18146 (0.02774)
WFG2 (3)	0.82249 (0.05295)	0.290 (0)	**0.84511 (0.04901)**	0.200	0.363 (0)	0.82624 (0.07204)
WFG4 (3)	**0.75439 (0.00157)**	0.096 (0)	0.75384 (0.00168)	0.100	0.600 (0)	0.75356 (0.00196)
WFG1 (4)	**1.42160 (0.00817)**	**0.000 (1)**	1.40961 (0.01053)	0.149	0.695 (0)	1.40913 (0.01532)
WFG2 (4)	0.79654 (0.18094)	0.610 (0)	0.77826 (0.24272)	0.300	0.684 (0)	**0.83725 (0.14104)**
WFG4 (4)	**1.03315 (0.00390)**	**0.038 (1)**	1.03063 (0.00256)	0.000	0.261 (0)	1.03104 (0.00351)
WFG1 (5)	**1.57620 (0.00699)**	**0.000 (1)**	1.56965 (0.00953)	0.124	0.492 (0)	1.56630 (0.01272)
WFG2 (5)	0.73478 (0.34582)	0.706 (0)	**0.84962 (0.19778)**	0.500	0.171 (0)	0.72441 (0.31308)
WFG4 (5)	**1.27679 (0.00434)**	0.154 (0)	1.27413 (0.00379)	0.127	0.446 (0)	1.27441 (0.00578)

TABLE 4. Results obtained by iSMS-EMOA, iSMS-EMOA II, and iSMS-EMOA-ARA with respect to the number of computations (N_{CHv}) of the hypervolume indicator. We present the percentage of saving computations of C_{Hv}. We show average values over 30 independent runs. The values in parentheses correspond to the standard deviations.

f	iSMS-EMOA	iSMS-EMOA II min N_{CHv}		iSMS-EMOA-ARA
	Saving N_{CHv}	Saving N_{CHv}	p_{rsi}	Saving N_{CHv}
DTLZ1 (3)	0.00% (0.000)	**25.93% (0.048)**	0.222	16.47% (1.282)
DTLZ2 (3)	0.00% (0.000)	26.92% (0.067)	0.193	**28.23% (0.129)**
DTLZ4 (3)	0.00% (0.000)	**32.66% (0.023)**	0.020	28.26% (0.102)
DTLZ7 (3)	0.00% (0.000)	**30.00% (0.040)**	0.100	25.95% (0.385)
DTLZ1 (4)	0.00% (0.000)	**28.53% (0.058)**	0.144	20.02% (0.707)
DTLZ2 (4)	0.00% (0.000)	**30.84% (0.033)**	0.075	28.39% (0.115)
DTLZ4 (4)	0.00% (0.000)	**33.33% (0.000)**	0.000	28.55% (0.109)
DTLZ7 (4)	0.00% (0.000)	**29.77% (0.053)**	0.107	26.53% (0.326)
DTLZ1 (5)	0.00% (0.000)	**25.33% (0.073)**	0.240	21.63% (0.577)
DTLZ2 (5)	0.00% (0.000)	**30.39% (0.041)**	0.088	28.41% (0.089)
DTLZ4 (5)	0.00% (0.000)	27.20% (0.054)	0.184	**28.63% (0.117)**
DTLZ7 (5)	0.00% (0.000)	**29.99% (0.043)**	0.100	26.65% (0.212)
WFG1 (3)	0.00% (0.000)	20.00% (0.066)	0.400	**27.02% (0.207)**
WFG2 (3)	0.00% (0.000)	**26.67% (0.067)**	0.200	24.49% (0.514)
WFG4 (3)	0.00% (0.000)	**30.00% (0.049)**	0.200	28.64% (0.121)
WFG1 (4)	0.00% (0.000)	**28.36% (0.049)**	0.149	26.51% (0.180)
WFG2 (4)	0.00% (0.000)	23.31% (0.050)	0.300	**25.58% (0.479)**
WFG4 (4)	0.00% (0.000)	**33.33% (0.000)**	0.000	28.37% (0.135)
WFG1 (5)	0.00% (0.000)	**29.19% (0.062)**	0.124	26.42% (0.236)
WFG2 (5)	0.00% (0.000)	16.68% (0.076)	0.500	**26.02% (0.415)**
WFG4 (5)	0.00% (0.000)	**29.09% (0.057)**	0.127	28.11% (0.178)

in most test problems, iSMS-EMOA II had to be executed several times by EVOCA (for each MOP under consideration) and then the required computational time was even greater than the original iSMS-EMOA. Conversely, it is interesting to see that iSMS-EMOA-ARA can adjust the value of p_{rsi} during the search to obtain good results (considering both to achieve a good quality of solutions and to minimize the calculations of the hypervolume contributions). Therefore, we can conclude that iSMS-EMOA-ARA is a good alternative to solve MOPs, particularly in high-dimensional objective spaces.

So far, we have compared the proposed iSMS-EMOA-ARA regarding iSMS-EMOA and iSMS-EMOA II. However, it could be interesting to compare the performance of the proposed algorithm regarding the original SMS-EMOA

TABLE 5. Results obtained by GDE3, MOEA/D-DE, NSGA3, SMS-EMOA and our iSMS-EMOA-ARA regarding I_{Hv}. We show average values over 30 independent runs. The values in parentheses correspond to the standard deviations. $P(H)$ shows the results of statistical analysis applied to our experiments using Wilcoxon's rank sum and considering I_{Hv}. P is the probability of observing that the null hypothesis "medians are equal" is true. $H = 1$ indicates that the null hypothesis can be rejected at the 5% level.

f	GDE3		MOEA/D-DE		NSGA3		SMS-EMOA		iSMS-EMOA-ARA
	I_{Hv}	$P(H)$	I_{Hv}	$P(H)$	I_{Hv}	$P(H)$	I_{Hv}	$P(H)$	I_{Hv}
DTLZ1 (3)	0.000 (0.000)	**0.000 (1)**	0.811 (0.412)	**0.000 (1)**	1.046 (0.016)	**0.000 (1)**	**1.123 (0.000)**	0.623 (0)	**1.123 (0.000)**
DTLZ2 (3)	0.540 (0.027)	**0.000 (1)**	0.661 (0.005)	**0.000 (1)**	0.693 (0.006)	**0.000 (1)**	**0.758 (0.000)**	0.956 (0)	**0.758 (0.000)**
DTLZ4 (3)	0.577 (0.017)	**0.000 (1)**	0.626 (0.109)	**0.000 (1)**	0.586 (0.170)	**0.000 (1)**	**0.758 (0.000)**	0.100 (0)	**0.758 (0.000)**
DTLZ7 (3)	0.000 (0.000)	**0.000 (1)**	0.133 (0.043)	**0.000 (1)**	0.188 (0.063)	**0.000 (1)**	0.529 (0.057)	**0.000 (1)**	**0.557 (0.038)**
DTLZ1 (4)	0.000 (0.000)	**0.000 (1)**	0.882 (0.497)	**0.000 (1)**	1.134 (0.023)	**0.000 (1)**	**1.374 (0.000)**	0.119 (0)	**1.374 (0.000)**
DTLZ2 (4)	0.198 (0.028)	**0.000 (1)**	0.755 (0.014)	**0.000 (1)**	0.808 (0.016)	**0.000 (1)**	**1.045 (0.000)**	**0.000 (1)**	1.044 (0.000)
DTLZ4 (4)	0.421 (0.048)	**0.000 (1)**	0.782 (0.036)	**0.000 (1)**	0.678 (0.202)	**0.000 (1)**	**1.045 (0.000)**	**0.000 (1)**	1.044 (0.000)
DTLZ7 (4)	0.000 (0.000)	**0.000 (1)**	0.000 (0.003)	**0.000 (1)**	0.076 (0.088)	**0.000 (1)**	0.578 (0.033)	0.056 (0)	**0.590 (0.030)**
DTLZ1 (5)	0.000 (0.000)	**0.000 (1)**	0.896 (0.545)	**0.000 (1)**	1.182 (0.020)	**0.000 (1)**	1.360 (0.164)	**0.000 (1)**	**1.568 (0.000)**
DTLZ2 (5)	0.551 (0.071)	**0.000 (1)**	1.000 (0.018)	**0.000 (1)**	0.987 (0.026)	**0.000 (1)**	1.418 (0.004)	**0.000 (1)**	**1.449 (0.000)**
DTLZ4 (5)	0.259 (0.058)	**0.000 (1)**	0.568 (0.302)	**0.000 (1)**	0.663 (0.219)	**0.000 (1)**	1.251 (0.005)	**0.000 (1)**	**1.297 (0.000)**
DTLZ7 (5)	0.076 (0.014)	**0.000 (1)**	0.788 (0.073)	**0.000 (1)**	0.682 (0.452)	**0.000 (1)**	1.078 (0.209)	**0.000 (1)**	**1.302 (0.005)**
WFG1 (3)	0.404 (0.015)	**0.000 (1)**	0.616 (0.022)	**0.000 (1)**	**1.087 (0.021)**	**0.000 (1)**	0.209 (0.011)	**0.000 (1)**	0.194 (0.013)
WFG2 (3)	1.041 (0.019)	**0.000 (1)**	1.029 (0.052)	**0.000 (1)**	**1.093 (0.079)**	**0.000 (1)**	0.186 (0.035)	0.701 (0)	0.193 (0.032)
WFG4 (3)	0.470 (0.010)	**0.000 (1)**	0.539 (0.010)	**0.000 (1)**	0.637 (0.010)	**0.000 (1)**	**0.755 (0.002)**	**0.005 (1)**	0.753 (0.002)
WFG1 (4)	0.533 (0.011)	**0.000 (1)**	0.714 (0.030)	**0.000 (1)**	**1.020 (0.108)**	**0.000 (1)**	0.328 (0.001)	**0.000 (1)**	0.323 (0.002)
WFG2 (4)	0.907 (0.035)	**0.000 (1)**	1.034 (0.062)	**0.000 (1)**	**1.168 (0.087)**	**0.000 (1)**	0.126 (0.023)	0.631 (0)	0.131 (0.021)
WFG4 (4)	0.552 (0.009)	**0.000 (1)**	0.633 (0.011)	**0.000 (1)**	0.670 (0.058)	**0.000 (1)**	**1.035 (0.003)**	**0.000 (1)**	1.030 (0.004)
WFG1 (5)	0.356 (0.012)	**0.000 (1)**	0.595 (0.034)	**0.000 (1)**	**0.972 (0.150)**	**0.000 (1)**	0.101 (0.007)	**0.000 (1)**	0.149 (0.002)
WFG2 (5)	**1.043 (0.029)**	**0.000 (1)**	1.023 (0.097)	**0.000 (1)**	1.013 (0.280)	**0.000 (1)**	0.161 (0.031)	**0.000 (1)**	0.170 (0.031)
WFG4 (5)	0.623 (0.012)	**0.000 (1)**	0.675 (0.015)	**0.000 (1)**	0.559 (0.212)	**0.000 (1)**	1.134 (0.012)	**0.000 (1)**	**1.267 (0.006)**

(which is one of the most popular hypervolume-based EMOAs) and other EMOAs based on different principles. Thus, in our comparative study, we adopted three popular state-of-the-art evolutionary approaches:

- The third evolution step of generalized differential evolution (GDE3) [78], it is an EMOA based on Pareto optimality and crowding distance. GDE3 is an effective EMOA with a computational complexity per generation of $O(N \log^{M-1} N)$ [78] (where M denotes the number of objectives).
- The multi-objective evolutionary algorithm based on decomposition with differential evolution (MOEA/D-DE) [36], it is one of the most powerful EMOAs based on decomposition to deal with complicated MOPs. Considering a neighborhood size T, MOEA/D-DE has a computation complexity per generation of $O(TN)$ with probability δ and $O(N^2)$ with probability $1 - \delta$. Considering the standard parameter $\delta = 0.9$, the computational complexity of MOEA/D-DE becomes much lower than most of multi-objective approaches found in the literature [36].
- The third version of the non-dominating sorting genetic algorithm (NSGA3) [79], it is a recent MOEA based on Pareto optimality and reference vectors. It has a computational complexity per generation of $O(N^2 \log^{M-2} N)$ [79].

In all the algorithms, we employed the standard parameters suggested by their respective authors.

Since SMS-EMOA can take a long time (up to five hours) to approximate the Pareto front in problems having more than four objectives, we have only employed the exact computation of the hypervolume contributions in problems with at most, four objective functions. In the case of problems with five objectives, we used the strategy proposed in [65] to approximate the hypervolume contributions of a set of non-dominated solutions. Table 5 shows the results obtained by iSMS-EMOA-ARA and the adopted EMOAs regarding I_{Hv} indicator. In this experimental study, we also included a statistical analysis using Wilcoxon's rank sum to identify significant differences between the algorithms. From these tables, we can see that EMOAs based on the hypervolume indicator outperformed the EMOAs based on the other principles in all DTLZ test problems and WFG4 test problem. It is worth mentioning that SMS-EMOA and iSMS-EMOA-ARA had similar behavior in seven test problems. On the other hand, iSMS-EMOA-ARA was better than SMS-EMOA in eight problems meanwhile SMS-EMOA was better than iSMS-EMOA-ARA in six test problems. Since SMS-EMOA calculates the exact hypervolume contributions of each solution in the population, it had a high computational cost, even much greater than iSMS-EMOA. SMS-EMOA required at most 256 seconds to solve MOPs with three objective functions and at most, 2,610 seconds to solve MOPs with 4 objective functions. In another way, iSMS-EMOA required at most 7 seconds and 89 seconds to approximate the Pareto front of these problems, respectively. Regarding the other EMOAs, we can see that the proposed iSMS-EMOA-ARA is better than GDE3, MOEA/D-DE and NSGA3 in all DTLZ test problems including WFG4. Note besides that for WFG1 and WFG2, GDE3, MOEA/D-DE, and NSGA3 were better than the proposed iSMS-EMOA-ARA. However, they were also better than SMS-EMOA, it means that for these

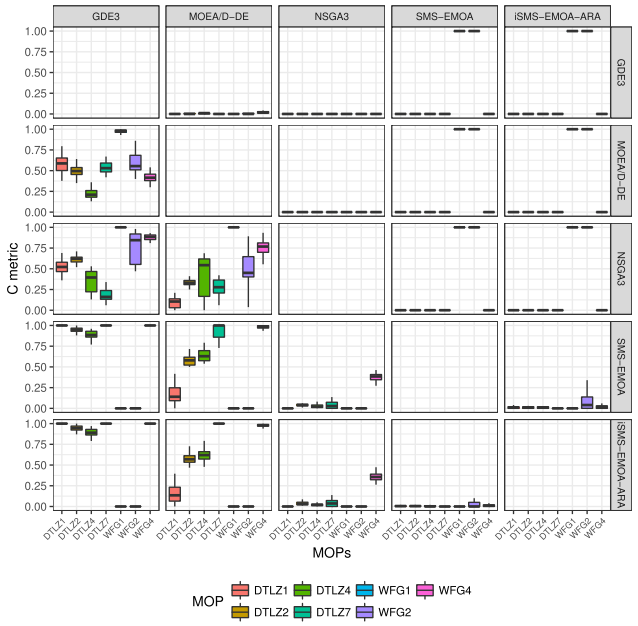

FIGURE 12. Two Set Coverage for GDE3, MOEA/D-DE, NSGA3, SMS-EMOA and our iSMS-EMOA-ARA on the three-objective test problems.

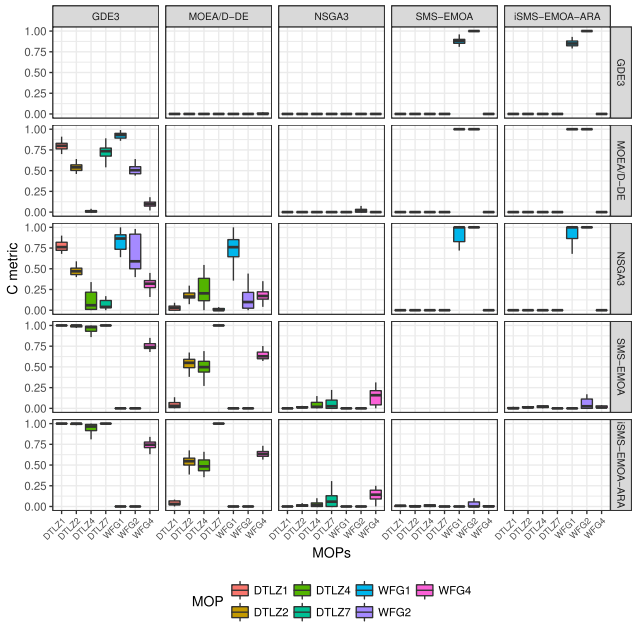

FIGURE 13. Two Set Coverage for GDE3, MOEA/D-DE, NSGA3, SMS-EMOA and our iSMS-EMOA-ARA on the four-objective test problems.

test problems the environmental selection mechanism based on I_{Hv} indicator was not a good alternative to deal with these problems. Instead, it is suggested the use of decomposition-based approaches which obtained better results.

The comparison among iSMS-EMOA, iSMS-EMOA II, and iSMS-EMOA-ARA, was only carried out by using the hypervolume indicator because these three EMOAs are based on this indicator, and then, the comparison is fair. However, when we compare GDE3, MOEA/D-DE, NSGA3, SMS-EMOA, and iSMS-EMOA-ARA, it is desirable the use of another indicator to corroborates the performance of any algorithm. In order to compare the quality of Pareto front approximations (in terms of dominance relation) between pairs of EMOAs, we employed the binary $\mathcal{C}$ metric (or set two coverage). Figs. 12–14 show the results of the evaluation with the performance measure $\mathcal{C}$. In order to illustrate the general performance of the algorithms in comparison, simple box plots are shown. The thick line represents the median value, the upper and lower ends of the box are the upper and lower quartiles, and the ends of the vertical line are minimum and maximum values, respectively. We computed the $\mathcal{C}$ metric by comparing pairs of algorithms (i.e., $\mathcal{C}(A, B)$ and $\mathcal{C}(B, A)$). These values were obtained as average values of the comparisons of all independent runs of algorithm A with all independent runs of algorithm B. In the charts, we show the ratio of solutions produced by iSMS-EMOA-ARA that dominate the solutions produced by GDE3, MOEA/D-DE, NSGA3, and SMS-EMOA, respectively. Each plot must be read as $\mathcal{C}(A, B)$, where A denotes the algorithm in the row, and B the algorithm in the column. Fig. 12 shows the results obtained by the EMOAs in problems with three objectives. From this plot, we can see that iSMS-EMOA-ARA obtained a better ratio of solutions that dominate those produced by GDE3 and

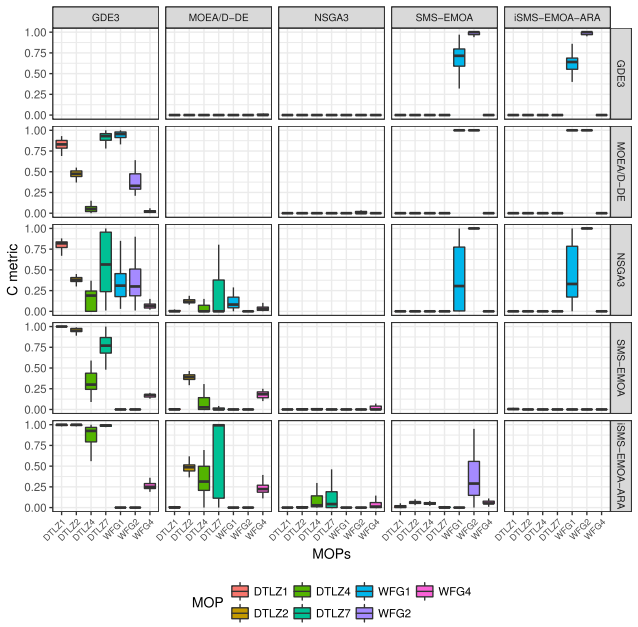

FIGURE 14. Two Set Coverage for GDE3, MOEA/D-DE, NSGA3, SMS-EMOA and our iSMS-EMOA-ARA on the five-objective test problems.

MOEA/D-DE in most of the test problems. However, for NSGA3 and SMS-EMOA, the quality of solutions (in terms of Pareto relation) became very similar. This behavior is also similar in problems with four objectives. iSMS-EMOA-ARA achieved a better ratio of solutions that dominate the solutions produced by GDE3 and MOEA/D-DE. Regarding NSGA3 and SMS-EMOA, the performance of the propose iSMS-EMOA-ARA become similar in terms of $\mathcal{C}$ metric. The same behavior can be observed for problems with five objectives. It is worth noticing that when the number of

TABLE 6. Results obtained by GDE3, MOEA/D-DE, NSGA3, SMS-EMOA and our iSMS-EMOA-ARA regarding I_{Hv}. We show average values over 30 independent runs. The values in parentheses correspond to the standard deviations. $P(H)$ shows the results of statistical analysis applied to our experiments using Wilcoxon's rank sum and considering I_{Hv}. P is the probability of observing that the null hypothesis "medians are equal" is true. $H = 1$ indicates that the null hypothesis can be rejected at the 5% level.

f	GDE3		MOEA/D-DE		NSGA3		SMS-EMOA		iSMS-EMOA ARA
	I_{Hv}	$P(H)$	I_{Hv}	$P(H)$	I_{Hv}	$P(H)$	I_{Hv}	$P(H)$	I_{Hv}
RW1 (3)	0.991 (0.006)	**0.000 (1)**	0.981 (0.011)	**0.000 (1)**	0.248 (0.078)	**0.000 (1)**	1.030 (0.010)	**0.000 (1)**	**1.037 (0.003)**
RW2 (4)	0.710 (0.018)	**0.000 (1)**	0.751 (0.009)	**0.000 (1)**	0.298 (0.116)	**0.000 (1)**	**0.821 (0.000)**	**0.000 (1)**	0.811 (0.003)

objectives increases, the ratio of solutions dominated by any algorithm decreases. It does not mean that the algorithms decrease their performance. When the values of $\mathcal{C}(A, B)$ and $\mathcal{C}(B, A)$ are almost the same, and they are small, it means that both algorithms are competitive regarding Pareto dominance relation.

VII. TWO REAL-WORLD ENGINEERING PROBLEMS FROM PRACTICE

After solving a number of test problems, we now apply the proposed algorithm to a couple of engineering optimization problems. Below, we describe the engineering problems adopted in our comparative study.

A. CASE STUDY I: CRASH-WORTHINESS DESIGN OF VEHICLES

The crash-worthiness design (CWD) problem of vehicles aims to optimize the frontal structure of a vehicle for crash-worthiness [80]. The thickness of five reinforced members $(t_1, \ldots, t_5)$ around the frontal structure is chosen as design variables. The multi-objective formulation of the problem consists of: i) minimize the *"mass of vehicle"* (*Mass*); ii) minimize the *deceleration during the "full frontal crash"* (A_{in}), which is proportional to biomechanical injuries caused to the occupants; and iii) minimize the *"toe board intrusion"* (*Intrusion*) in the "offset-frontal crash", which accounts for the structural integrity of the vehicle. Thus, the box-constrained multi-objective optimization problem is written as

$$\begin{aligned} &\textbf{minimize: } f_1(\mathbf{x}) = Mass \\ &\textbf{minimize: } f_2(\mathbf{x}) = A_{in} \\ &\textbf{minimize: } f_3(\mathbf{x}) = Intrusion \end{aligned} \tag{5}$$

where $\mathbf{x} = (t_1, t_2, t_3, t_4, t_5)^\intercal$, such that $1mm \leq t_i \leq 3mm$, for $i \in \{1, \ldots, 5\}$. The mathematical formulation for the three objectives can be found in the original study [80].

B. CASE STUDY II: LIQUID-ROCKET SINGLE ELEMENT INJECTOR DESIGN

Liquid-rocket single element injector design (LSEID) problem has two primary goals: to improve its performance and to enlarge its life [81]. A proper injector design can achieve such goals. According to Vaidyanathan *et al.* [82], the objectives to be considered for an optimal injector design consist of: i) minimize the distance from the inlet "*combustion length*" (X_{cc}), where 99% of the combustion is complete; ii) minimize the maximum temperature of the injector face, *"face temperature"* (TF_{max}); iii) minimize wall temperature at 3in (fourth probe) from the injector face *"wall temperature"* (TW_4); and iv) minimize the maximum temperature on the post tip of the injector *"tip temperature"* (TT_{max}). In its original formulation [82], the LSEID problem considers the above four objectives. More precisely, the box-constrained many-objective optimization problem can be written as:

$$\begin{aligned} &\textbf{minimize: } f_1(\mathbf{x}) = X_{cc} \\ &\textbf{minimize: } f_2(\mathbf{x}) = TF_{max} \\ &\textbf{minimize: } f_3(\mathbf{x}) = TW_4 \\ &\textbf{minimize: } f_4(\mathbf{x}) = TT_{max} \end{aligned}$$

where $\mathbf{x} = (\alpha, \Delta HA, \Delta OA, OPTT)^T$, such that α is the *"hydrogen flow angle"* varying between 0° to 20°; ΔHA is the *"hydrogen area"* increment with respect to the baseline cross-section area (0.0186 in^2) (increment varies from 0% to 25% of the baseline hydrogen area); ΔOA denotes the *oxygen area* decrement with respect to the baseline cross-section area (0.0423 in^2) of the tube carrying oxygen (the area varies between 0% and (-40)% of the baseline area); and *OPTT* is the *oxidizer post tip thickness* which varies between X'' to $2X''$, where X'' is the tip thickness with a baseline value 0.01 in. The mathematical formulation of the four objectives can be found in [81].

C. ANALYSIS OF RESULTS

In Table 6 we show the numerical values found by the EMOAs concerning the hypervolume indicator. As can be seen, the proposed iSMS-EMOA-ARA obtained a higher hypervolume value than all the EMOAs under comparison in the crash-worthiness design problem, i.e., CWD problem. It means that the non-dominated solutions found by iSMS-EMOA-ARA reached a better convergence and spread along the PF. Moreover, iSMS-EMOA-ARA significantly outperformed all the EMOAs adopted in our comparative study according to Wilcoxon's rank sum test with a p-value of 0.05. However, for the liquid-rocket single element injector design problem, i.e., LSEID problem, the best performance was achieved by SMS-EMOA. Although in this real-world problem our proposed approach became significantly better than GDE3, MOEA/D-DE, and NSGA3, iSMS-EMOA-ARA was outperformed considerably by SMS-EMOA. However, it is

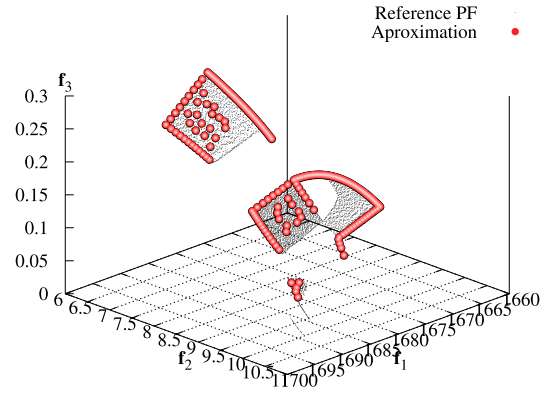

FIGURE 15. Pareto front approximation achieved by iSMS-EMOA-ARA in the CWD problem.

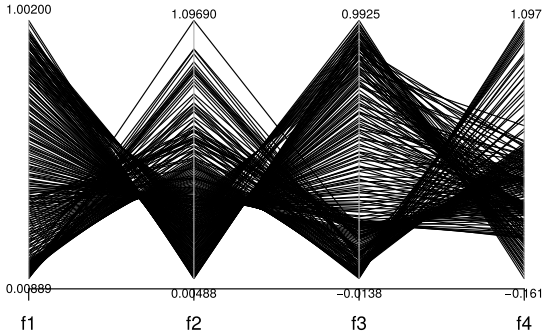

FIGURE 16. Parallel coordinates achieved by iSMS-EMOA-ARA for the LSEID problem.

worth recalling that SMS-EMOA needs more computational effort than iSMS-EMOA-ARA.

It is worth noticing that the hypervolume-based approaches (i.e., SMS-EMOA and iSMS-EMOA-ARA) achieved a better performance than the EMOAs based on different principles. This remark suggests that hypervolume-based EMOAs can adapt in a better way the shape of the Pareto front, i.e., most of the Pareto front was adequately covered by these two approaches. Fig. 15 shows the Pareto front approximation achieved by iSMS-EMOA in the CWD problem, while that the parallel plots in Fig. 16 give an idea of the objective space regions covered by iSMS-EMOA in the LSEID problem.

VIII. CONCLUSIONS

Hypervolume-based EMOAs are an attractive alternative to solve MOPs because of two main reasons: (i) hypervolume indicator is Pareto compliant, and hence, maximizing it yields a good-quality approximation of the Pareto front of a MOP, and (ii) it does not need extra information, which is especially important in real-world applications where the features of the problem are unknown. Arguably, the main disadvantage of this type of EMOAs is that we cannot compute the hypervolume indicator in polynomial time. For this reason, some researchers aim to reduce the number of hypervolume computations. In this work, we have proposed an adaptative control strategy to reduce the number of hypervolume contributions per iteration of a hypervolume-based EMOA. We compared iSMS-EMOA-ARA against its predecessors: iSMS-EMOA and iSMS-EMOA II employing standard benchmark test problems taken from the DTLZ and WFG test suites. According to results, we observed that iSMS-EMOA-ARA obtained good-quality approximate Pareto fronts, saving up to 28 percent of the hypervolume computations. This means that iSMS-EMOA-ARA achieved to adjust the value of p_{rsi} successfully. We also compared iSMS-EMOA-ARA against the original SMS-EMOA and other three EMOAs based on different principles: GDE3, MOEA/D-DE, and NSGA3 using the same test problems. iSMS-EMOA-ARA achieved a better performance than SMS-EMOA in the most problems, and it required much lower computational time. Regarding GDE3, MOEA/D-DE and NSGA3, iSMS-EMOA-ARA was the best EMOA in DTLZ test problems including WFG4 test problem. For WFG1 and WFG2 test problems, GDE3, MOEA/D-DE, and NSGA3 were better than iSMS-EMOA-ARA. However, they were also better than the original SMS-EMOA and then we concluded that these two problems are difficult for hypervolume-based EMOAs.

Finally, we evaluated the proposed approach on two engineering problems: Crash-Worthiness Design of Vehicles (CWD) and Liquid-rocket Single Element Injector Design (LSEID). In the CWD problem, iSMS-EMOA-ARA was better than SMS-EMOA, GDE, MOEA/D-DE and NSGA3. In the case of the LSEID problem, iSMS-EMOA-ARA was better than GDE, MOEA/D-DE, and NSGA3 but SMS-EMOA was better than iSMS-EMOA-ARA. However, it is worth recalling that SMS-EMOA has a higher computational cost that iSMS-EMOA-ARA. Therefore, iSMS-EMOA-ARA is a promising alternative for solving problems with a high number of objectives. As a conclusion, we can say that the proposed approach is an excellent alternative to deal with multi-objective optimization problems for three main reasons: i) it is competitive with respect to state-of-the-art EMOAs based on hypervolume, ii) it does not need extra information of the problem (which is particularly essential when solving real-world applications) and iii) its computational cost is much lower than the other hypervolume-based EMOAs. As part of our future work, it is desirable to explore other ways to adjust p_{rsi}, in iSMS-EMOA-ARA, during the search process. We also consider exploring different selection schemes to be used into iSMS-EMOA. We hypothesized that to use a neighborhood of solutions in the environmental selection scheme of iSMS-EMOA-ARA could improve the quality of results. However, this fact will increase the computational cost of the algorithm. Nonetheless, this is in fact, a possible path for future research.

REFERENCES

[1] C. A. C. Coello, "A comprehensive survey of evolutionary-based multiobjective optimization techniques," *Knowl. Inf. Syst.*, vol. 1, no. 3, pp. 269–308, 1999.
[2] A. Zhou, B.-Y. Qu, H. Li, S.-Z. Zhao, P. N. Suganthan, and Q. Zhang, "Multiobjective evolutionary algorithms: A survey of the state of the art," *Swarm Evol. Comput.*, vol. 1, no. 1, pp. 32–49, 2011.
[3] N. Nedjah and L. de Macedo Mourelle, "Evolutionary multi–objective optimisation: A survey," *Int. J. Bio-Inspired Comput.*, vol. 7, no. 1, pp. 1–25, 2015.

[4] K. Deb, A. Pratap, S. Agarwal, and T. Meyarivan, "A fast and elitist multiobjective genetic algorithm: NSGA-II," *IEEE Trans. Evol. Comput.*, vol. 6, no. 2, pp. 182–197, Apr. 2002.

[5] E. Zitzler, M. Laumanns, and L. Thiele, "SPEA2: Improving the strength Pareto evolutionary algorithm," in *Proc. Evol. Methods Design, Optim. Control Appl. Ind. Problems (EUROGEN)*, Athens, Greece, K. Giannakoglou, D. Tsahalis, J. Periaux, P. Papailou, and T. Fogarty, Eds., 2002, pp. 95–100.

[6] H. Ishibuchi and T. Murata, "A multi-objective genetic local search algorithm and its application to flowshop scheduling," *IEEE Trans. Syst., Man, Cybern. C, Appl. Rev.*, vol. 28, no. 3, pp. 392–403, Aug. 1998.

[7] A. Jaszkiewicz, "On the performance of multiple-objective genetic local search on the 0/1 knapsack problem—A comparative experiment," *IEEE Trans. Evol. Comput.*, vol. 6, no. 4, pp. 402–412, Aug. 2002.

[8] Q. Zhang and H. Li, "MOEA/D: A multiobjective evolutionary algorithm based on decomposition," *IEEE Trans. Evol. Comput.*, vol. 11, no. 6, pp. 712–731, Dec. 2007.

[9] R. Cheng, Y. Jin, K. Narukawa, and B. Sendhoff, "A multiobjective evolutionary algorithm using Gaussian process-based inverse modeling," *IEEE Trans. Evol. Comput.*, vol. 19, no. 6, pp. 838–856, Dec. 2015.

[10] E. Zitzler and S. Künzli, "Indicator-based selection in multiobjective search," in *Parallel Problem Solving from Nature—PPSN VIII* (Lecture Notes in Computer Science), vol. 3242, X. Yao, Ed. Birmingham, U.K.: Springer-Verlag, 2004, pp. 832–842.

[11] N. Beume, B. Naujoks, and M. Emmerich, "SMS-EMOA: Multiobjective selection based on dominated hypervolume," *Eur. J. Oper. Res.*, vol. 181, no. 3, pp. 1653–1669, 2007.

[12] E. Zitzler and L. Thiele, "Multiobjective optimization using evolutionary algorithms—A comparative case study," in *Parallel Problem Solving from Nature—PPSN V*, A. E. Eiben, Ed. Amsterdam, The Netherlands: Springer-Verlag, 1998, pp. 292–301.

[13] M. P. Hansen and A. Jaszkiewicz, "Evaluating the quality of approximations to the non-dominated set," Dept. Math. Model., Tech. Univ. Denmark, Lyngby, Denmark, Tech. Rep. IMM-REP-1998-7, Mar. 1998.

[14] E. Zitzler, L. Thiele, M. Laumanns, C. M. Fonseca, and V. G. D. Fonseca, "Performance assessment of multiobjective optimizers: An analysis and review," *IEEE Trans. Evol. Comput.*, vol. 7, no. 2, pp. 117–132, Apr. 2003.

[15] C. A. C. Coello and M. R. Sierra, "A study of the parallelization of a coevolutionary multi-objective evolutionary algorithm," in *Proc. 3rd Mexican Int. Conf. Artif. Intell. (MICAI)*, in Lecture Notes in Artificial Intelligence, vol. 2972, R. Monroy, G. Arroyo-Figueroa, L. E. Sucar, and H. Sossa, Eds. Berlin, Germany: Springer-Verlag, Apr. 2004, pp. 688–697.

[16] C. A. R. Villalobos and C. A. C. Coello, "A new multi-objective evolutionary algorithm based on a performance assessment indicator," in *Proc. ACM GECCO*, 2012, pp. 505–512.

[17] C. Domínguez-Medina, G. Rudolph, O. Schütze, and H. Trautmann, "Evenly spaced Pareto fronts of quad-objective problems using PSA partitioning technique," in *Proc. IEEE CEC*, Jun. 2013, pp. 3190–3197.

[18] S. Z. Martínez, V. A. S. Hernández, H. Aguirre, K. Tanaka, and C. A. C. Coello, "Using a family of curves to approximate the Pareto front of a multi-objective optimization problem," in *Proc. 13th Int. Conf. Parallel Problem Solving Nature—PPSN XIII*, Ljubljana, Slovenia, in Lecture Notes in Computer Science, vol. 8672, T. Bartz-Beielstein, J. Branke, B. Filipič, and J. Smith, Eds. Cham, Switzerland: Springer, Sep. 2014, pp. 682–691.

[19] L. M. Antonio and C. A. C. Coello, "Indicator-based cooperative coevolution for multi-objective optimization," in *Proc. IEEE Congr. Evol. Comput. (CEC)*, Vancouver, BC, Canada. Piscataway, NJ, USA: IEEE Press, Jul. 2016, pp. 991–998.

[20] K. Bringmann and T. Friedrich, "Approximating the least hypervolume contributor: NP-hard in general, but fast in practice," in *Proc. 5th Int. Conf. Evol. Multi-Criterion Optim. (EMO)*, Nantes, France, in Lecture Notes in Computer Science, vol. 5467, M. Ehrgott, C. M. Fonseca, X. Gandibleux, J.-K. Hao, and M. Sevaux, Eds. Berlin, Germany: Springer, Apr. 2009, pp. 6–20.

[21] N. Tsukamoto, Y. Sakane, Y. Nojima, and H. Ishibuchi, "Incorporation of hypervolume approximation with scalarizing functions into indicator-based evolutionary multiobjective optimization algorithms," *Trans. Inst. Syst., Control Inf. Eng.*, vol. 23, pp. 165–177, Jan. 2010.

[22] J. Bader, K. Deb, and E. Zitzler, "Faster hypervolume-based search using Monte Carlo sampling," in *Multiple Criteria Decision Making for Sustainable Energy and Transportation Systems* (Lecture Notes in Economics and Mathematical Systems), vol. 634, M. Ehrgott, B. Naujoks, T. J. Stewart, and J. Wallenius, Eds. Heidelberg, Germany: Springer, 2010, pp. 313–326.

[23] K. Tagawa, H. Shimizu, and H. Nakamura, "Indicator-based differential evolution using exclusive hypervolume approximation and parallelization for multi-core processors," in *Proc. ACM Genet. Evol. Comput. Conf. (GECCO)*, Dublin, Ireland, Jul. 2011, pp. 657–664.

[24] S. Jiang, J. Zhang, Y.-S. Ong, A. N. Zhang, and P. S. Tan, "A simple and fast hypervolume indicator-based multiobjective evolutionary algorithm," *IEEE Trans. Cybern.*, vol. 45, no. 10, pp. 2202–2213, Oct. 2015.

[25] F. Y. Edgeworth, *Mathematical Physics*. London, U.K.: P. Keagan, 1881.

[26] V. Pareto, *Cours D'Économie Politique*. Lausanne, Switzerland: F. Rouge, 1896.

[27] D. E. Goldberg, *Genetic Algorithms in Search, Optimization and Machine Learning*. Reading, MA, USA: Addison-Wesley, 1989.

[28] N. Srinivas and K. Deb, "Multiobjective optimization using nondominated sorting in genetic algorithms," *Evol. Comput.*, vol. 2, no. 3, pp. 221–248, Dec. 1994.

[29] K. Deb and D. E. Goldberg, "An investigation of niche and species formation in genetic function optimization," in *Proc. 3rd Int. Conf. Genet. Algorithms*, J. D. Schaffer, Ed. San Mateo, CA, USA: Morgan Kaufmann, Jun. 1989, pp. 42–50.

[30] M. Farina and P. Amato, "On the optimal solution definition for many-criteria optimization problems," in *Proc. Int. Conf. NAFIPS-FLINT*, Piscataway, NJ, USA, Jun. 2002, pp. 233–238.

[31] A. Farhang-Mehr and S. Azarm, "Diversity assessment of Pareto optimal solution sets: An entropy approach," in *Proc. Congr. Evol. Comput. (CEC)*, Piscataway, NJ, USA, vol. 1, May 2002, pp. 723–728.

[32] N. Hallam, P. Blanchfield, and G. Kendall, "Handling diversity in evolutionary multiobjective optimization," in *Proc. IEEE Congr. Evol. Comput. (CEC)*, Scotland, U.K., vol. 3, Sep. 2005, pp. 2233–2240.

[33] S. B. Gee, K. C. Tan, V. A. Shim, and N. R. Pal, "Online diversity assessment in evolutionary multiobjective optimization: A geometrical perspective," *IEEE Trans. Evol. Comput.*, vol. 19, no. 4, pp. 542–559, Aug. 2015.

[34] M. Li, S. Yang, and X. Liu, "Diversity comparison of Pareto front approximations in many-objective optimization," *IEEE Trans. Cybern.*, vol. 44, no. 12, pp. 2568–2584, Dec. 2014.

[35] H. Wang, Y. Jin, and X. Yao, "Diversity assessment in many-objective optimization," *IEEE Trans. Cybern.*, vol. 47, no. 6, pp. 1510–1522, Jun. 2017.

[36] H. Li and Q. Zhang, "Multiobjective optimization problems with complicated Pareto sets, MOEA/D and NSGA-II," *IEEE Trans. Evol. Comput.*, vol. 13, no. 2, pp. 284–302, Apr. 2009.

[37] Q. Zhang, W. Liu, and H. Li, "The performance of a new version of MOEA/D on CEC09 unconstrained MOP test instances," in *Proc. IEEE Congr. Evol. Comput.*, May 2009, pp. 203–208.

[38] H. Li, Q. Zhang, and J. Deng, "Multiobjective test problems with complicated Pareto fronts: Difficulties in degeneracy," in *Proc. IEEE Congr. Evol. Comput. (CEC)*, Beijing, China. Piscataway, NJ, USA: IEEE Press, Jul. 2014, pp. 2156–2163.

[39] S. Zapotecas-Martínez, C. A. C. Coello, H. E. Aguirre, and K. Tanaka, "A review of features and limitations of existing scalable multiobjective test suites," *IEEE Trans. Evol. Comput.*, to be published, doi: 10.1109/TEVC.2018.2836912.

[40] H. Ishibuchi, Y. Setoguchi, H. Masuda, and Y. Nojima, "Performance of decomposition-based many-objective algorithms strongly depends on Pareto front shapes," *IEEE Trans. Evol. Comput.*, vol. 21, no. 2, pp. 169–190, Apr. 2017.

[41] T. Okabe, Y. Jin, and B. Sendhoff, "A critical survey of performance indices for multi-objective optimisation," in *Proc. Congr. Evol. Comput. (CEC)*, Canberra, ACT, Australia, vol. 2. Piscataway, NJ, USA: IEEE Press, Dec. 2003, pp. 878–885.

[42] S. Jiang, Y.-S. Ong, J. Zhang, and L. Feng, "Consistencies and contradictions of performance metrics in multiobjective optimization," *IEEE Trans. on*, vol. 44, no. 12, pp. 2391–2404, Dec. 2014.

[43] O. Schütze, X. Esquivel, A. Lara, and C. A. C. Coello, "Using the averaged Hausdorff distance as a performance measure in evolutionary multiobjective optimization," *IEEE Trans. Evol. Comput.*, vol. 16, no. 4, pp. 504–522, Aug. 2012.

[44] E. M. Lopez and C. A. C. Coello, "IGD$^+$-EMOA: A multi-objective evolutionary algorithm based on IGD$^+$," in *Proc. IEEE Congr. Evol. Comput. (CEC)*, Jul. 2016, pp. 999–1006.

[45] D. Brockhoff, T. Wagner, and H. Trautmann, "2 indicator-based multiobjective search," *Evol. Comput.*, vol. 23, no. 3, pp. 369–395, 2015.

[46] R. H. Gómez and C. A. C. Coello, "MOMBI: A new metaheuristic for many-objective optimization based on the R2 indicator," in *Proc. IEEE CEC*, Jun. 2013, pp. 2488–2495.

[47] D. H. Phan and J. Suzuki, "R2-IBEA: R2 indicator based evolutionary algorithm for multiobjective optimization," in *Proc. IEEE Congr. Evol. Comput.*, Jun. 2013, pp. 1836–1845.
[48] O. Schutze, A. Lara, and C. A. C. Coello, "On the influence of the number of objectives on the hardness of a multiobjective optimization problem," *IEEE Trans. Evol. Comput.*, vol. 15, no. 4, pp. 444–455, Aug. 2011.
[49] J. Knowles and D. Corne, "Properties of an adaptive archiving algorithm for storing nondominated vectors," *IEEE Trans. Evol. Comput.*, vol. 7, no. 2, pp. 100–116, Apr. 2003.
[50] S. Huband, P. Hingston, L. While, and L. Barone, "An evolution strategy with probabilistic mutation for multi-objective optimisation," in *Proc. Congr. Evol. Comput. (CEC)*, Canberra, ACT, Australia, vol. 3. Piscataway, NJ, USA: IEEE Press, Dec. 2003, pp. 2284–2291.
[51] M. Emmerich, N. Beume, and B. Naujoks, "An EMO algorithm using the hypervolume measure as selection criterion," in *Proc. 3rd Int. Conf. Evol. Multi-Criterion Optim. (EMO)*, Guanajuato, Mexico, in Lecture Notes in Computer Science, vol. 3410, C. A. C. Coello, A. H. Aguirre, and E. Zitzler, Eds. Berlin, Germany: Springer, Mar. 2005, pp. 62–76.
[52] C. Igel, N. Hansen, and S. Roth, "Covariance matrix adaptation for multi-objective optimization," *Evol. Comput.*, vol. 15, no. 1, pp. 1–28, 2007.
[53] N. Hansen, "The CMA evolution strategy: A comparing review," in *Towards a New Evolutionary Computation*, J. Lozano, P. Larranaga, I. Inza, and E. Bengoetxea, Eds. Berlin, Germany: Springer, 2006, pp. 75–102.
[54] S. Mostaghim, J. Branke, and H. Schmeck, "Multi-objective particle swarm optimization on computer grids," in *Proc. Genet. Evol. Comput. Conf. (GECCO)*, vol. 1, D. Thierens, Ed. London, U.K., Jul. 2007, pp. 869–875.
[55] S. Zapotecas-Martínez, A. López-Jaimes, and A. García-Nájera, "LIBEA: A Lebesgue indicator-based evolutionary algorithm for multi-objective optimization," *Swarm Evol. Comput.*, to be published. [Online]. Available: https://orcid.org/0000-0002-1690-3875, doi: 10.1016/j.swevo.2018.05.004.
[56] J. D. Knowles, "Local-search and hybrid evolutionary algorithms for Pareto optimization," Ph.D. dissertation, Dept. Comput. Sci., Univ. Reading, Reading, U.K., Jan. 2002.
[57] C. M. Fonseca, L. Paquete, and M. Lopez-Ibanez, "An improved dimension-sweep algorithm for the hypervolume indicator, " in *Proc. IEEE Congr. Evol. Comput. (CEC)*, Vancouver, BC, Canada, Jul. 2006, pp. 3973–3979.
[58] L. M. S. Russo and A. P. Francisco, "Quick hypervolume," *IEEE Trans. Evol. Comput.*, vol. 18, no. 4, pp. 481–502, Aug. 2014.
[59] L. While, L. Bradstreet, and L. Barone, "A fast way of calculating exact hypervolumes," *IEEE Trans. Evol. Comput.*, vol. 16, no. 1, pp. 86–95, Feb. 2012.
[60] L. Bradstreet, L. Barone, and L. While, "Updating exclusive hypervolume contributions cheaply," in *Proc. IEEE Congr. Evol. Comput. (CEC)*, Trondheim, Norway. Piscataway, NJ, USA: IEEE Press, May 2009, pp. 538–544.
[61] K. Bringmann and T. Friedrich, "An efficient algorithm for computing hypervolume contributions," *Evol. Comput.*, vol. 18, no. 3, pp. 383–402, 2010.
[62] M. T. M. Emmerich and C. M. Fonseca, "Computing hypervolume contributions in low dimensions: Asymptotically optimal algorithm and complexity results," in *Proc. 6th Int. Conf. Evol. Multi-Criterion Optim. (EMO)*, Ouro Preto, Brazil, in Lecture Notes in Computer Science, vol. 6576, R. H. Takahashi, K. Deb, E. F. Wanner, and S. Greco, Eds. Berlin, Germany: Springer, Apr. 2011, pp. 121–135.
[63] W. Cox and L. While, "Improving the IWFG algorithm for calculating incremental hypervolume," in *Proc. IEEE Congr. Evol. Comput. (CEC)*, Jul. 2016, pp. 3969–3976.
[64] K. Bringmann and T. Friedrich, "Approximating the volume of unions and intersections of high-dimensional geometric objects," *Comput. Geometry*, vol. 43, nos. 6–7, pp. 601–610, 2010.
[65] J. Bader and E. Zitzler, "HypE: An algorithm for fast hypervolume-based many-objective optimization," *Evol. Comput.*, vol. 19, no. 1, pp. 45–76, Mar. 2011.
[66] H. Ishibuchi, N. Tsukamoto, Y. Sakane, and Y. Nojima, "Hypervolume approximation using achievement scalarizing functions for evolutionary many-objective optimization," in *Proc. IEEE Congr. Evol. Comput. (CEC)*, Trondheim, Norway. Piscataway, NJ, USA: IEEE Press, May 2009, pp. 530–537.
[67] H. Ishibuchi, N. Tsukamoto, Y. Sakane, and Y. Nojima, "Indicator-based evolutionary algorithm with hypervolume approximation by achievement scalarizing functions," in *Proc. ACM 12th Annu. Conf. Genet. Evol. Comput. (GECCO)*, Portland, OR, USA, Jul. 2010, pp. 527–534.
[68] A. Menchaca-Mendez and C. A. C. Coello, "A new selection mechanism based on hypervolume and its locality property," in *Proc. IEEE Congr. Evol. Comput. (CEC)*, Cancún, Mexico. Piscataway, NJ, USA: IEEE Press, Jun. 2013, pp. 924–931.
[69] A. Auger, J. Bader, D. Brockhoff, and E. Zitzler, "Theory of the hypervolume indicator: Optimal μ-distributions and the choice of the reference point," in *Proc. 10th ACM SIGEVO Workshop Found. Genet. Algorithms (FOGA)*, Orlando, FL, USA, Jan. 2009, pp. 87–102.
[70] A. Menchaca-Mendez, E. Montero, M.-C. Riff, and C. A. C. Coello, "A more efficient selection scheme in iSMS-EMOA," in *Proc. 14th Ibero-Amer. Conf. Adv. Artif. Intell. (IBERAMIA)*, Santiago de Chile, Chile, in Lecture Notes in Artificial Intelligence, vol. 8864, A. L. Bazzan and K. Pichara, Eds. Cham, Switzerland: Springer, Nov. 2014, pp. 371–380.
[71] M.-C. Riff and E. Montero, "A new algorithm for reducing metaheuristic design effort," in *Proc. IEEE Congr. Evol. Comput. (CEC)*, Cancún, Mexico, Jun. 2013, pp. 3283–3290.
[72] K. Deb, L. Thiele, M. Laumanns, and E. Zitzler, "Scalable test problems for evolutionary multiobjective optimization," in *Evolutionary Multiobjective Optimization*, A. Abraham, L. Jain, and R. Goldberg, Eds. London, U.K.: Springer, 2005, pp. 105–145.
[73] S. Huband, P. Hingston, L. Barone, and L. While, "A review of multiobjective test problems and a scalable test problem toolkit," *IEEE Trans. Evol. Comput.*, vol. 10, no. 5, pp. 477–506, Oct. 2006.
[74] A. Blot, H. H. Hoos, L. Jourdan, M.-É. Kessaci-Marmion, and H. Trautmann, "MO-ParamILS: A multi-objective automatic algorithm configuration framework," in *Proc. 10th Int. Conf. Learn. Intell. Optim. (LION)*, Ischia, Italy, P. Festa, M. Sellmann, and J. Vanschoren, Eds. Cham, Switzerland: Springer, May/Jun. 2016, pp. 32–47.
[75] E. Montero, M.-C. Riff, and B. Neveu, "A beginner's guide to tuning methods," *Appl. Soft Comput.*, vol. 17, pp. 39–51, Apr. 2014.
[76] F. Hutter, H. H. Hoos, K. Leyton-Brown, and T. Stützle, "ParamILS: An automatic algorithm configuration framework," *J. Artif. Int. Res.*, vol. 36, pp. 267–306, Sep. 2009.
[77] E. Zitzler, K. Deb, and L. Thiele, "Comparison of multiobjective evolutionary algorithms: Empirical results," *Evol. Comput.*, vol. 8, no. 2, pp. 173–195, 2000.
[78] S. Kukkonen and J. Lampinen, "GDE3: The third evolution step of generalized differential evolution," in *Proc. IEEE Congr. Evol. Comput. (CEC)*, Scotland, U.K., vol. 1, Sep. 2005, pp. 443–450.
[79] K. Deb and H. Jain, "An evolutionary many-objective optimization algorithm using reference-point-based nondominated sorting approach, part I: Solving problems with box constraints," *IEEE Trans. Evol. Comput.*, vol. 18, no. 4, pp. 577–601, Aug. 2014.
[80] X. Liao, Q. Li, X. Yang, W. Zhang, and W. Li, "Multiobjective optimization for crash safety design of vehicles using stepwise regression model," *Struct. Multidisciplinary Optim.*, vol. 35, no. 6, pp. 561–569, 2008.
[81] T. Goel, R. Vaidyanathan, R. T. Haftka, W. Shyy, N. V. Queipo, and K. Tucker, "Response surface approximation of Pareto optimal front in multi-objective optimization," *Comput. Methods Appl. Mech. Eng.*, vol. 196, pp. 879–893, Jan. 2007.
[82] R. Vaidyanathan, P. K. Tucker, N. Papila, and W. Shyy, "Computational-fluid-dynamics-based design optimization for single-element rocket injector," *J. Propuls. Power*, vol. 20, no. 4, pp. 705–717, 2004.

ADRIANA MENCHACA-MÉNDEZ received the M.Sc. and Ph.D. degrees in computer science from CINVESTAV-IPN, Mexico, in 2008 and 2015, respectively. She has been a Professor with ENES Campus Morelia, National Autonomous University of Mexico, Morelia, since 2016. She has published 13 technical papers in international conferences and journals. Her current research interests include multi-objective evolutionary optimization, hypervolume-based multi-objective evolutionary algorithms, combinatorial optimization, and parameter setting problems. She has also served as a reviewer of different international journals and conferences in the field of evolutionary computation.

ELIZABETH MONTERO (M'08) received the Ph.D. degree from the University of Nice-Sophia Antipolis, France. She is currently a Professor in computing science with Universidad Andres Bello, Chile. She has published over 30 technical papers in high-level heuristic search conferences, such as GECCO, PPSN, and CEC. Her research interests include the foundations and application of heuristic search methods, parameter setting problems, and applications to combinatorial optimization.

SAÚL ZAPOTECAS-MARTÍNEZ (M'10) received the M.Sc. and Ph.D. degrees in computer science from CINVESTAV-IPN, Mexico, in 2007 and 2013, respectively. He was an Assistant Professor with the Department of Electrical and Electronic Engineering, Shinshu University, Nagano, Japan, from 2014 to 2016. Since 2017, he has been a Visiting Professor with the Department of Applied Mathematics and Systems, Universidad Autónoma Metropolitana Unidad Cuajimalpa, Ciudad de México, Mexico. He has authored or co-authored over 40 technical papers and book chapters. His current research interests include multi-objective evolutionary optimization, multi-objective benchmarking, and expensive multi-objective optimization. He is a member of the ACM. His publications currently report over 300 citations in Google Scholar, and his H-index is 11. He has served in the program committee of several international conferences and as a reviewer of several international journals in the field of evolutionary computation.